Production Well Performance Enhancement using Sonication Technology

Technical Progress Report for the Period 03/25/2002 to 03/24/2003

By

Michael A. Adewumi, M. Thaddeus Ityokumbul, Robert W. Watson,
Mario Farías, Glenn Heckman, Johnson Olanrewaju, Eltohami Eltohami, and Bruce G. Miller,
Department of Energy and GeoEnvironmental Engineering/The Energy Institute; and

W. Jack Hughes and Thomas C. Montgomery,
Applied Research Laboratory

December 17, 2003

Work Performed Under Cooperative Agreement No. DE-FC26-02NT15187

For
NETL AAD Document Control, Bldg. 921
U.S. Department of Energy
National Energy Technology Laboratory
P.O. Box 10940
Pittsburgh, Pennsylvania 15236-0940

By
Department of Energy and GeoEnvironmental Engineering/ The Energy Institute
The Pennsylvania State University
C211 Coal Utilization Laboratory
University Park, Pennsylvania 16802

DISCLAIMER

ABSTRACT

The objective of this project is to develop a sonic well performance enhancement technology that focuses on near wellbore formations. In order to successfully achieve this objective, a three-year project has been defined with each year consisting of four tasks. The first task is the laboratory-scale study whose goal is to determine the underlying principles of the technology. The second task will develop a scale-up mathematical model to serve as the design guide for tool development. The third task is to develop effective transducers that can operate with variable frequency so that the most effective frequencies can be applied in any given situation. The system, assembled as part of the production string, ensures delivery of sufficient sonic energy to penetrate the near-wellbore formation. The last task is the actual field testing of the tool. The first year of the project has been completed.

Task 1. Laboratory-Scale Experiments

In Task 1, a literature review of laboratory and field investigations employing acoustic stimulation to enhance fluid flow in porous media was performed. Two characteristics appear to be common to most of the previous work reported. One is lack of systematic data that may be truly classified as scientific, and the other, is inconsistency in the empirical evidence offers as to the impact of elastic waves on oil recovery from petroleum reservoirs.

The findings from the literature review were used to design our experimental protocol. A slim-tube experimental system was designed to enable us to perform systematic studies on the interaction of elastic waves with fluids in porous media. Experiments performed during the first year focused on determining the inception of cavitation, studying thermal dissipation under cavitation conditions, investigating sonic energy interactions with glass beads and oil, and studying the effects of sonication on crude oil properties.

Our initial focus was on determining the operation characteristics of transducers with the goals of delineating the conditions for the onset of cavitation and determining the power dissipation rate during cavitation since we believe that sonic stimulation will

be enhanced when the device is operated under cavitation conditions. Our findings show that the voltage threshold for onset of cavitation is independent of transducer-hydrophone separation distance.

Thermal dissipation under cavitation conditions was studied because energy dissipation may promote the mobilization of deposited paraffins and waxes. Our preliminary laboratory experiments suggest that waxes are mobilized when the fluid temperature approaches 40°C.

Studies were performed investigating the interaction of sonic energy with glass beads in water, with oil droplets in water, and core samples. The tests with glass beads and oil in water provided phenomenal information with respect to movement, coalescence, and effect on composition. Acoustic energy drove off the lighter fractions, aromatics, and branched alkanes.

Task 2. Development of a Computer Model for Scale-Up

The primary efforts towards the simulation of the effect of sonication on the near-wellbore region have focused on the development of a numerical model for handling the transportation of fluids under the influence of strong sonic waves in the porous medium. Governing equations describing this type of fluid transport process have not been adequately presented in the literature, and hence significant effort was directed at doing this as part of Task 2. Activities included developing the numerical framework, developing accurate algorithm solutions, and validating the code.

Task 3. Development of a New Generation of Acoustic Transducers

Past systematic investigations of flow-enhanced parameters are poorly defined and irreproducible. The reproducibility of these experiments may be difficult, if not impossible, due to insufficient information. The need to understand the governing mechanisms of acoustic energy-fluid-solid interactions in porous media requires versatile transducers that can be operated within various parameters. In this task, experiments were performed to gain insight into these interactions and provide information to design a slim-tube apparatus for performing the experiments. The design of this apparatus was

performed during the first year of the project. Results from the testing, to be performed during the second year, will then be used to design the tool for field testing.

Task 4. Field Testing of the Sonication Technology

The overall plan for this task is to perform field trials of the sonic transducer design. The trials will be performed in production and/or injection wells located in Pennsylvania, New York, and West Virginia. Work during the first year included performing literature searches, meeting with producers to schedule testing, gathering production information, cores, and samples from wells, and drilling four new wells for use in the project.

TABLE OF CONTENTS

1.0 Introduction

The need for drilling new wells to increase domestic production has dominated the energy sufficiency debate for the last 30 years. This often suppresses the fact that there are millions of existing wells with a great deal of potential for enhancing production if wellbore hydraulics can be rendered more favorable. These wells are not producing at their full capacity because of flow restrictions caused by the near-wellbore formation damage. Their potential can be turned to production capacity with availability of appropriate technology. Marginal well operators, which number hundreds of thousands, cannot afford to deploy conventional technologies. Development and deployment of the right technology will improve productivity and add significantly to the nation's oil and gas resources. Flow inhibition into the wellbore may be caused by any or a combination of the following:

- solids deposition through production operations (e.g., wax, paraffin, scales, asphaltenes, hydrates, salt);
- near-wellbore effects (e.g., perforation damage, tunnel damage);
- invasion of drilling fluids and solids;
- condensate banking;
- unfavorable phase distribution (e.g., Joule-Thompson effect); and
- fines migration.

Traditionally, a number of techniques have been applied to remediate wellbore damage and enhance productivity. These include mechanical methods (e.g. scraping), chemical injection (e.g. paraffin dispersants and acids), and thermal methods (e.g. hot oil treatment). Although these technologies are mature, they have inherent disadvantages that include high initial and disposal costs, potential environmental degradation, and safety issues. Sonic technology has the potential to be an effective means of oil well productivity enhancement without negative side effects.

The objective of this project is to develop a sonic well performance enhancement technology that focuses on near wellbore formations. In order to successfully achieve this objective, a three-year project has been defined with each year consisting of four tasks. The first task is the laboratory-scale study whose goal is to determine the underlying principles of the technology. The second task will develop a scale-up mathematical model to serve as the design guide for tool development. The third task is to develop effective transducers that can operate with variable frequency so that the most effective frequencies can be applied in any given situation. The system, assembled as part of the production string, ensures delivery of sufficient sonic energy to penetrate the near-wellbore formation. The last task is the actual field testing of the tool.

The principal goals of this project are to:

1) develop a mechanistic understanding of the enhancement impact of sonic energy on oil well productivity; and
2) develop a suitable downhole sonic device that can be deployed in the field to enhance oil well productivity through near-wellbore flow improvement.

The first year of the project has been completed and the technical progress and status are summarized in Section 2.0. Section 3.0 contains the detailed description of the plans for the second year of the project. References are contained in Section 4.0.

2.0 Technical Progress and Status of Year 1 Activities

2.1 Task 1. Laboratory-Scale Experiments

2.1.1 Introduction

A literature review of laboratory and field investigations employing acoustic stimulation to enhance fluid flow in porous media was carried out (see Appendix A). The findings from this review were used to design our experimental protocol. Preliminary experiments to elucidate the interaction of sonic energy with light and heavey crude oil samples in fluid-fluid and fluid-solid systems were carried out. The results of these studies are presented and discussed.

2.1.2 Acoustic Excitation of Fluids in Porous Media: A Summary

Empirical observations reported in the literature have indicated that immediately following a natural seismic activity there was a significant increase in the production of crude oil and water from numerous fields in the vicinity of the seismic activity. As a result of these observations, several laboratory and field studies have been carried out in an attempt to understand how acoustic energy enhances fluid flow in porous media. The effects of seismic activities were especially pronounced near inactive anticline faults. While quantitative data supporting these claims were not provided, field data have shown that under certain conditions, sonic stimulation promoted well productivity. However, the converse has also been observed; therefore research is clearly needed to delineate favorable regimes for the application of sonic stimulation in oil production.

A review of the literature suggests that the probable mechanisms for flow enhancement with sonic stimulation may be related to:

- Removal of paraffin (waxes) and asphaltenes near the wellbore;
- Increased oil coalescence and apparent permeability; and

- Reductions in oil viscosity and/or interfacial tension.

Two characteristics appear to be common to most of the previous work reported. One is lack of systematic data that may be truly classified as scientific, and the other, are inconsistencies in the empirical evidence offered as to the impact of elastic waves on oil recovery from petroleum reservoirs. Thus, in cases where improvements were noticed, a cognant scientific explanation as to what mechanism may be responsible is lacking, and similarly there are no explanations for the cases of failure. As a result, there is no established set of criteria, based on scientific studies, to discriminate between reservoirs for which this method might be appropriate and the ones for which it might not apply. The goal of this study is to provide a body of scientific knowledge to evaluate and characterize sonic flooding as a viable method for improving oil recovery. The database of scientific information developed would allow one to evolve the mechanisms for this novel acoustic excitation and utilize the database as the basis for the development of design and operating models.

2.1.3 Design of the Slip-Tube Set-Up

A slim-tube experimental system has been designed to enable us to perform systematic studies on the interaction of elastic waves with fluids in porous media. The design of the set-up is similar to that used by scientists at the Los Alamos National Laboratory (Venkitaraman et al., 1994) with some modifications. For example, our design incorporates fluid chambers at both ends of the slim tube. This modification is expected to improve the coupling of the transducer head with the fluid. The length of each mixing chamber will be 25.4 mm and its diameter will be the same as that of the slim tube (25.4 mm). One of these chambers will house a 19-mm diameter sonic transducer for the generation of sound. Figure 1.1 shows a detailed design of the endcap housing the transducer. This design will be used to study both concurrent and countercurrent arrangements for sonic excitation and fluid flow. The operating parameters for the set-up are shown in Table 1.1.

The setup is designed for the inlet and effluent fluid lines to be interchanged when conducting experiments with sonic energy and fluid flow in either concurrent or countercurrent arrangements. Sensors (thermocouple, static pressure transducer and acoustic pressure sensors) are positioned at 76, 152, 300, 520 and 840 mm along the 900-mm long slim tube. In addition, the inlet and the effluent flow lines are fitted with pressure

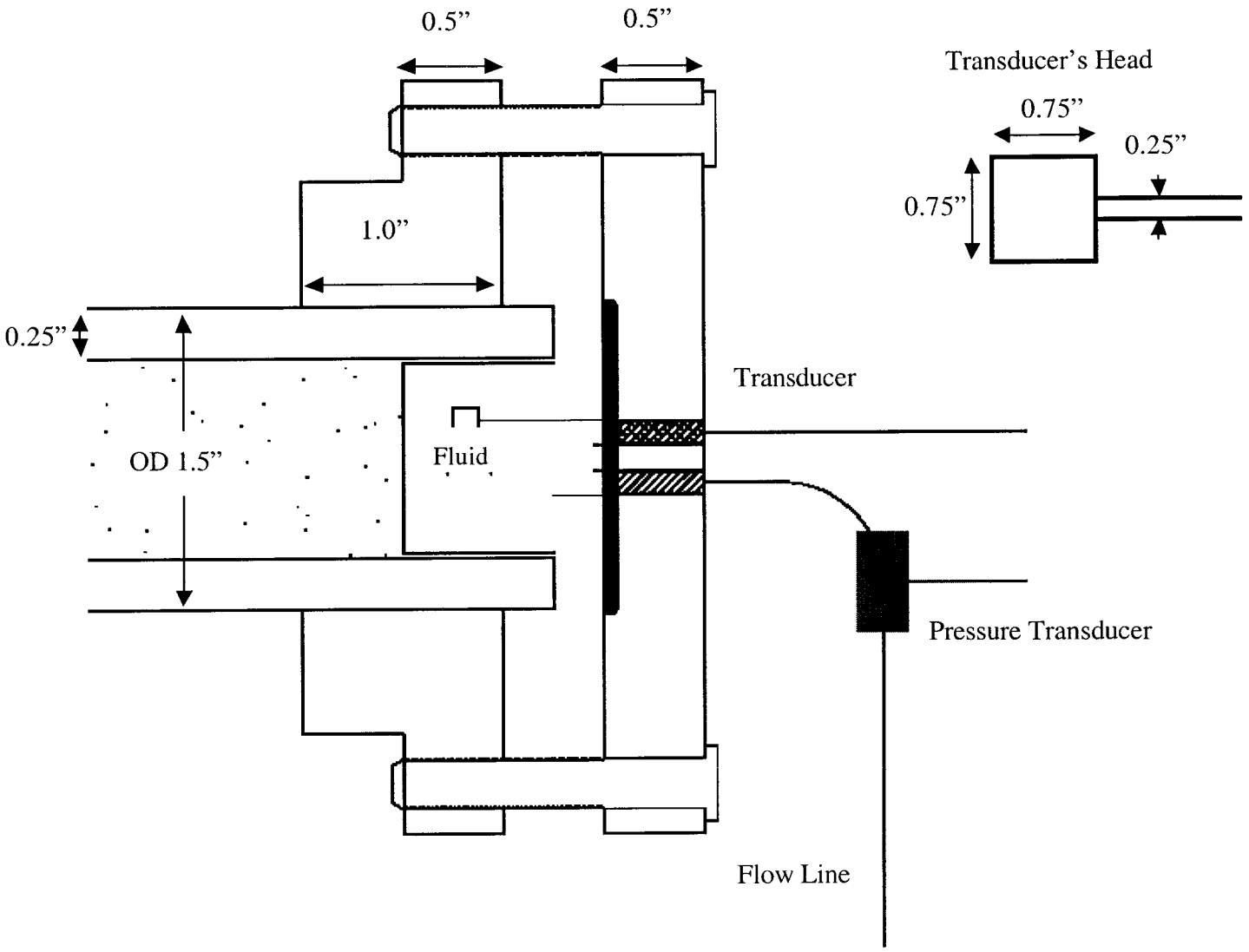

Figure 1.1 A detailed end-cap figure showing a transducer's head positioned in the 1" in diameter and 1" in length fluid chamber.

transducers to monitor pressure differentials at the two terminals. The clustering of the first three sensors is intended to elucidate changes in acoustic intensity in the vicinity of the transducer. Initial acoustic intensity, Io, near the tip of the transducer will be determined without the packing materials and the wave field intensity, I, spanning the length of the packing material will be measured and used to determine the effective penetration depth of the sonic excitation.

Table 1.1 Materials property required for a slim-tube apparatus

Material	**Criteria/factor for selection**
Transducer- sound wave source	frequency 100 Hz to 60 kHz; operating temperature 25 to100°C; pressure 600 psi; made of inert material; size: 0.75" diameter; removable.
Receiver (hydrophones)	frequency 100 Hz to 60 kHz; operating temperature 25 to100°C; pressure 600 psi or at initial burst pressure; made of inert material; millimeter size.
Stainless-steel tube	Variable lengths (8, 26, and 38"), ID 1" OD 1.5"; thickness 0.25"; operating temperature 25 to 100°C; 600 psi.
Mode of transducer operation	Continuous wave and pulse modes
Packing materials	Rounded and surface methylated glass beads, sand (silica), alumina particle size (mesh) 50-60, 60-70, 70-80, 80-100
Filter	Stainless-steel filter, low-acoustic impedance or thickness less than operating wavelength, pore size smaller than the smallest particle size
Sample collector	Interval timer and fraction collector

2.1.4 Preliminary Experiments and Results

For the preliminary experiments, the following equipment was used:

Function Generator- Hewlett Packard model 3314A. This equipment serves as power generator, inputs for power amplifier and the oscilloscope. Parameters such as frequency, amplitude, and duty cycles can be input and adjusted as needed.

Oscilloscope- Philips model PM 3261. It is mainly used as voltage and current readout of input/output signals from the power generator and output signals from the hydrophone. The amplitudes of the signals can be controlled by separate gain knobs.

Power Amplifier- Wilcoxon Research model PA7D. The power amplifier amplifies the AC voltage input from the generator and feeds it to the matching network.

Matching Network- Wilcoxon Research model N7C. The matching network is connected between the power amplifier and the transducer. By selecting various impendence taps on the transformer, the power factor to the transducer is matched so that more power can be sent to the transducer.

Transducers- Three Applied Research Laboratory (ARL)-fabricated transducers were supplied: two rated at 20 kHz and one at 40 kHz.

Hydrophones- Two polyvinyliden fluoride (PVDF) hydrophones were supplied by ARL. These hydrophones were fabricated and characterized in their laboratories. One of the hydrophones is rectangular in shape while the other is circular in shape and is 25.4 mm in diameter and thickness of 6.4 mm.

Shaker- Wilcoxon Research Shaker F4 Driver Serial 9681 with a nominal impedence of 10 Ohms. It is a ring-shaped shaker that can be attached to the test specimen via a mounting plug, piezoshaker, or impedance head. The power needed to drive the shaker is obtained from the power amplifier and matching network. The F4 shaker is suitable for pulse mode excitation operation. It is part of the components needed for the slim-tube experiments.

2.1.4.1 Determination of Cavitation Inception

Our initial focus was on determining the operational characteristics of the two transducers provided by ARL. Our goal was to delineate the conditions for the onset of cavitation. Our second goal was to determine the power dissipation rate during cavitation. In the special case where the near wellbore damage is due to deposition of waxes and/or asphaltenes, we believe that sonic stimulation will be enhanced when the device is operated under cavitation conditions. During cavitation, the energy dissipated is focused in a narrow zone and the heat generated may promote the mobility of the waxes and/or asphaltenes.

Procedure: The experimental setup used to determine the onset of cavitation is shown in Figure 1.2. A lead urethane (PU) block was suspended in a 3.5 L beaker filled with tap water from three chains attached to a hook. The hook was connected to a gear mechanism, which was used to alter the transducer-hydrophone separation distance. A hydrophone whose sensitivity was previously determined at ARL was attached to the top of the PU

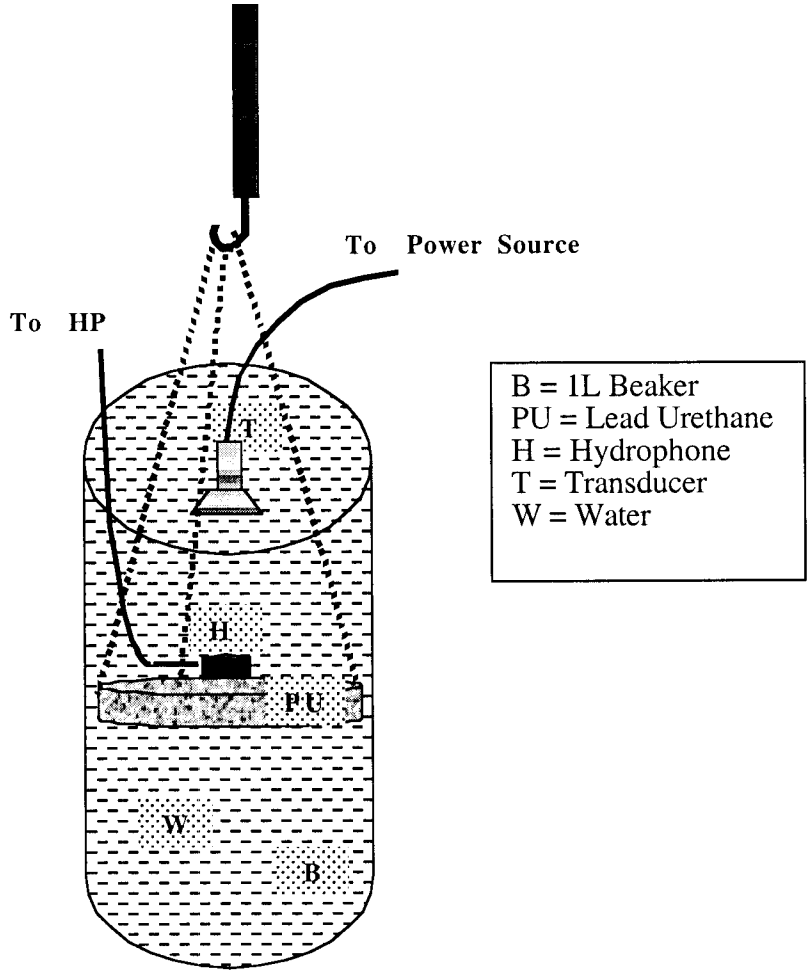

Figure 1.2 Experimental setup to elucidate sonic energy interaction with fluids

block and was connected to the HP Analyzer. The PU block used as an acoustic absorber to reduce standing wave nodes in the beake. During operation, the analyzer displays the operating frequency, hydrophone output drive level voltage (dB V_{rms}) and total harmonic distortion.

At a fixed frequency and transducer input drive voltage, the corresponding current was read from the oscilloscope. Sound pressure exerted on the hydrophone by the transducer was obtained from the HP Analyzer as receive drive level voltage. From the input drive voltage, the transducer's drive level voltage was calculated. The experimental conditions employed are shown below:

Matching network setting = 500 Vrms
Amplitude = 3.50 V (peak)
Power Amplifier = variable
Pulse length = 0.004 sec or Duty cycle 0.40%
Frequency: 20, 15, 10 and 5 kHz
Transducer head-hydrophone distance = 8, 12, or 16 cm

Using the hydrophone sensitivity curve and the measured receive drive level voltage, the sound pressure level (SPL) was calculated. To determine the onset of cavitation, the SPL is plotted as a function of the hydrophone drive level voltage. The break in the plot represents onset of cavitation. In general, the transducer-hydrophone separation did not have an effect over the SPL measurement over the range of 8-16 cm.

Results and Discussion: In order to determine the onset of cavitation, the SPL was plotted as a function of transmit drive level voltage. A typical plot is shown in Figure 1.3. The results show that at a fixed frequency, the SPL increases linearly with the receive drive level voltage with a break in the response observed at 35 drive level voltage. This break corresponds to the onset of cavitation when the transducer is operated at 20 kHz. These tests were repeated at different frequencies and the results for onset of cavitation are shown in Figure 1.4. In general, the drive level voltage threshold for onset of cavitation decreases with increasing frequency. A drop of about 4 dB was observed in the SPL when cavitation occurred. This indicates that a considerable amount of energy is concentrated in the cavitation phenomena. As indicated earlier, our findings show that the voltage threshold for onset of cavitation is independent of transducer-hydrophone separation distance.

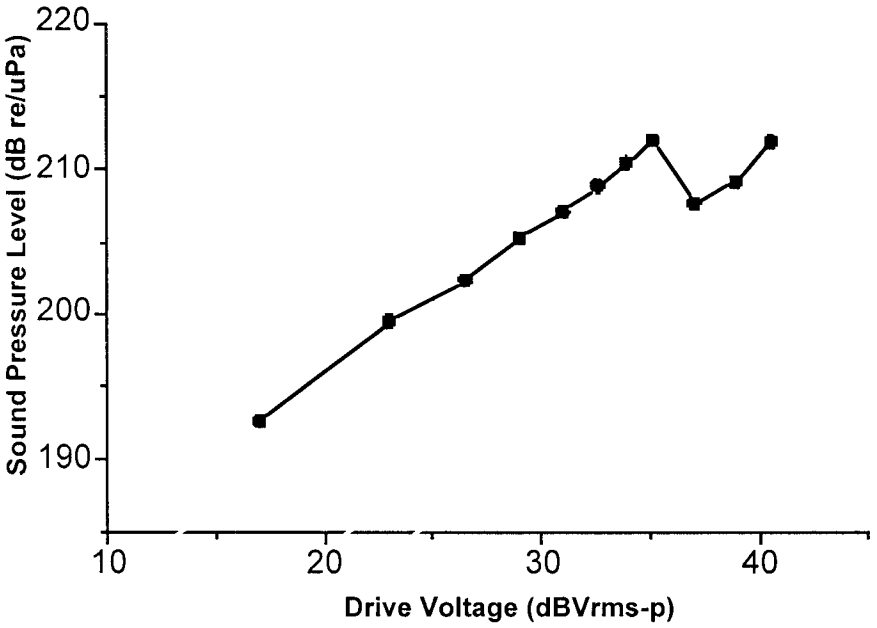

Figure 1.3 Linearity of pressure output with drive voltage, 20kHz, 0.004 sec pulse length

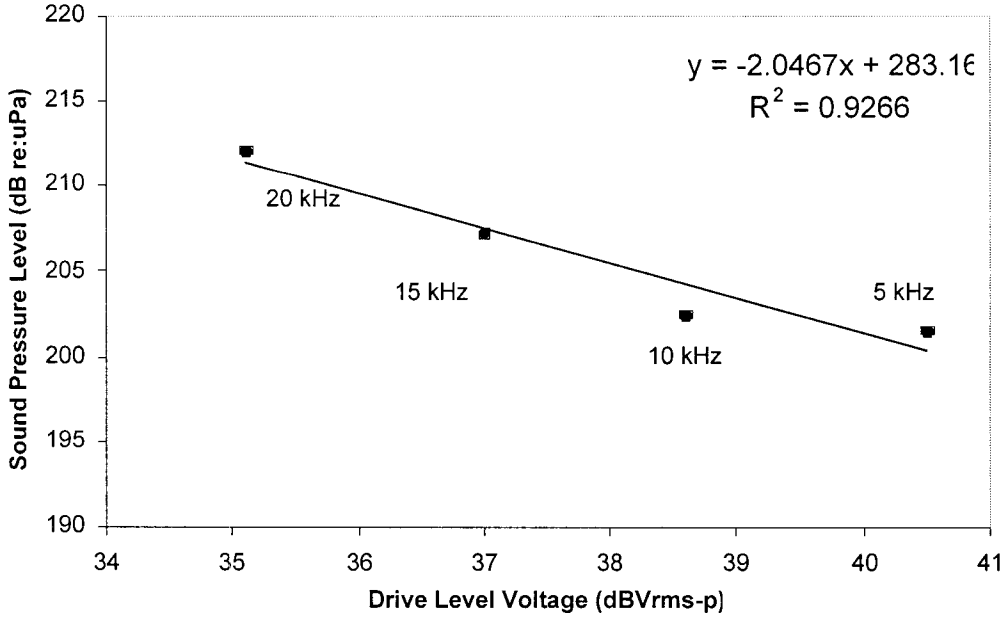

Figure 1.4 Cavitation threshold for different transducer frequencies

2.1.4.2 Thermal Dissipation Under Cavitation

Procedure: The experimental conditions are similar to those employed in determining the onset of cavitation with the exception that the power generator was set to 40% duty cycle and an amplitude of 3.50V. Three hundred milliliters of tap water, initially at 18°C, were put in a Styrofoam cup covered with a rubber disc. A digital thermocouple was inserted to record the temperature. The 20 kHz transducer was also inserted through the disc and partially submerged in the water. To avoid temperature gradients, the water in the container was stirred throughout the test. Power supply to the transducer was increased until cavitation conditions were reached. The variation of temperature with time was recorded. In order to investigate the possible effect of nucleation sites on power dissipation under cavitation, two teaspoons of glass beads (60-120 mesh) were added to 300 mL of tap water initially at 18°C and the experiment repeated.

Results and Discussion: Figure 1.5 shows the variation of water temperature with time. A regression analysis of the data gave a slope of approximately 0.31°C/min. It can be shown from theory that:

$$P = M C_p \frac{dT}{dt}$$

where P is the power dissipation rate, M, Cp and dT/dt are the mass and specific heat of water and slope of the plot, respectively. The results show that the presence of the solid particles did not have a significant affect on the response. From the slope of the response and the mass of water, the power dissipation is calculated to be 6.43 W. Since the transducer has a diameter of 1 cm, the specific power dissipation is determined to be approximately 82 kW/m^2.

It is obvious that the specific power dissipation rate was quite high even at such a low duty cycle. It is therefore possible that when deployed in a wellbore, the energy dissipation may promote the mobilization of deposited paraffins and waxes. Our laboratory experiments suggest the waxes are mobilized when the fluid temperature approaches 40°C. Additional experiments are planned to estimate the power dissipation at lower transducer operating frequencies.

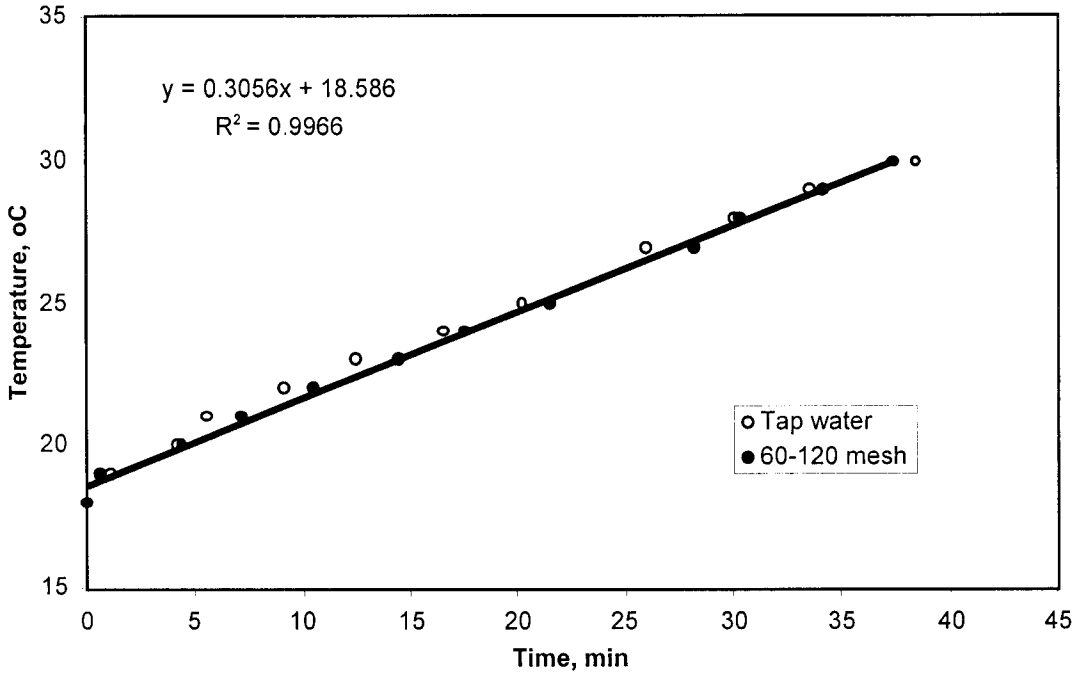

Figure 1.5 Variation of water temperature under cavitation

2.1.4.3 Sonic Energy Interaction with Glass Beads

Procedures: About 200 and 550 mL of water were poured into 250 and 600 mL beakers, respectively. Glass beads (60-120 mesh size) were added to the beakers with gentle agitation. The distances from the transducer's head to the bottom of the beaker were approximately 6 and 12 cm, respectively. The excited power was gradually increased until cavitation was attained.

Results: When the power was raised up to the cavitation level, the glass beads spread out. The fine bubbles that were generated collapsed or coalesced to form larger bubbles, which were attached to the glass beads. After about 5 minutes, some of the attached bubbles rose to the surface where they burst releasing their load of particles, which rained down to the bottom of the beaker. When power was turned off, several agglomerated bubbles with glass beads rose to the surface as well. However, some glass beads and bubble conglomerates did not rise but stayed at the bottom where they remained after 14 days of

observations. Since the glass beads are hydrophilic in nature, their recovery by the bubbles generated under cavitation conditions would suggest that the bubbles had a charge opposite that of the glass beads.

2.1.4.4 Sonic Energy Interaction with Oil

Procedure: One drop of used motor oil was dropped on a glass slide in air with the aid of a hypodermic syringe. The drop spread on the surface of the glass to a diameter of approximately 1 cm. The slide was carefully placed on the hydrophone immersed in water and resting on the lead-urethane polymer block. The power to the transducer was increased until cavitation conditions were reached.

Results: Initially, the oil was observed to break into several small droplets which moved around the transducer near field, coalesced and/or rose to the surface. The small oil droplets behaved like rigid spheres. However, with continuous sonic bombardment of the droplets, they coalesced into a big lump which remained intact even after sonic stimulation was turned off. A re-exposure of the glass slide to air resulted in an instantaneous spreading of the oil droplet. This observation would suggest that sonic excitation may promote oil coalescence by altering the oil interfacial tension. It is not clear at the present time if the behavior of the oil droplet is related to the release of certain components from the oil into the water. It is noted that during the excitation, a white fume-like cloud was released from the oil droplet into the water and was accompanied by a change in the physical appearance of the oil droplet (from a dark coloration to a grayish color). Additional experiments have been carried out using Pennsylvania paraffinic and other heavy crude oil sources with similar results.

2.1.4.5 Effect of Sonication on Properties of Crude Oil

As noted above, we observed that white fumes were released into the water when the oil droplet was excited with an attendant change in the color of the droplet. We extended this study by using Pennsylvania paraffinic and Colorado heavy crude oil samples on glass slides and/or core samples. A digital video of the phenomena was produced and shown at the DOE-sponsored Stripper Well Consortium meeting in Pittsburgh, Pennsylvania (November 12 and 13, 2002). The observation confirmed that under cavitation conditions, the oil initially breaks into smaller oil droplets which later coalesce and migrate on the

surface of the glass slide and/or core sample. Due to instability, the large oil droplets detach and rise to the surface of the water in the container.

We attempted to characterize the residue following sonic treatment. Specifically we wish to determine if any components of the oil are susceptible to sonic treatment. This information is required to establish if sonic treatment results in the production of oil with diminished or enhanced value – a factor that will impact the acceptability of the technology by oil producers. While we note that these tests were carried out in an environment where there was no confining pressure, it is nevertheless important to determine if gross changes in the oil properties results from the treatment. When the fabrication of the slim tube is completed, these tests will be repeated. For this test, we used a sample of Pennsylvania (PA) crude oil.

Procedure: A sample of PA crude oil was added to tap water and sealed in a plastic pipette-dropper. The pipette was put in water and irradiated with sonic energy. Power was increased until cavitation conditions were reached. The whole mixture turned milky with the application of sonic energy. At the end of the experiments, samples were kept undisturbed for several days. After the water was carefully removed, the oil residue in the tube was separated and prepared for GC-MS analysis.

A sample of oil residue was poured into a separatory funnel. Methylene chloride (CH_2Cl_2) was added to dissolve and concentrate the organic components. The mixture was shaken vigorously and occasionally vented to relief pressure buildup. The methylene chloride was transferred into a column containing anhydrous magnesium sulfate to remove any traces of water from the sample. The dried sample (eluent from the column) was collected in a 2 mL bottle. The aqueous phase and a sample of untreated PA crude were similarly prepared.

A Shimadzu Gas Chromatograph model GC-17A version 3 equipped with a Mass Spectrometer model QP-5000 and XTi-5 column was used for the chemical analysis. The column was 30-m long, 0.25mm ID and 0.25μm film thickness. An auto sampler (model AOC-20i) was used to inject the samples into the GC-MS which was operated using Class 5000 software. The temperature of the column was initially programmed to increase from 40 to 150°C at the rate of 10°C/minute. When the target temperature was reached, it was held there for 5 minutes. At the completion of this program, the temperature was gently raised from 150 to 300°C at a heating rate of 4°C/minute. The column was maintained at 300°C for 10 minutes. The MS data collection time spanned 4 to 63.5 minutes and

corresponded to 63.5 minutes total acquisition period. For these analyses, we used a scan rate of 1000 counts/minute for mass to charge ratio (m/z) in the range of 40 to 300.

Results and Discussion: Figure 1.6 show typical chromatograms of untreated PA crude oil and the residue obtained after sonic treatment. The concentrations of the organics in the aqueous phase were low and as such will not be discussed at this time. Efforts are underway to concentrate these species and the results will be reported at a later date. For the identification and integration of the peak areas, we used a gradient that was 1% of the maximum intensity observed for the scan. We used the Class 5000 software to match and identify the components present in the different sample. Tables 2.2 and 2.3 show the results from this match.

Our analysis confirms that the predominant species in the untreated crude oil were paraffins (mostly straight chain alkanes) with smaller quantities of branched alkanes and aromatic compounds. While the composition of the residue from the sonic treated samples was similar to that of the untreated crude oil, there were several differences. For example, the lighter fractions with low retention times were lost during the treatment as were the aromatic and branched alkanes. Since the aromatic components are not needed in the production of lubricants or gasoline fractions, their loss may be desirable. We note that in tests using the sealed pipette droppers, the tube appeared to be under vacuum. This would be indicative of the possible reaction of the oxygen trapped in the tube with the aromatic fraction. This observation would suggest that sonication may be a viable procedure for the treatment of organic wastes containing aromatic fractions.

2.2 Task 2. Development of a Computer Model for Scale-Up

2.2.1 Introduction

The primary efforts towards the simulation of the effect of sonication on the near-well region have focused on the development of a numerical model for handling the transportation of fluids under the influence of strong sonic waves in the porous medium. Governing equations describing this type of fluid transport processes have not been adequately presented in the literature, and hence significant effort is being directed at doing this as part of this task.

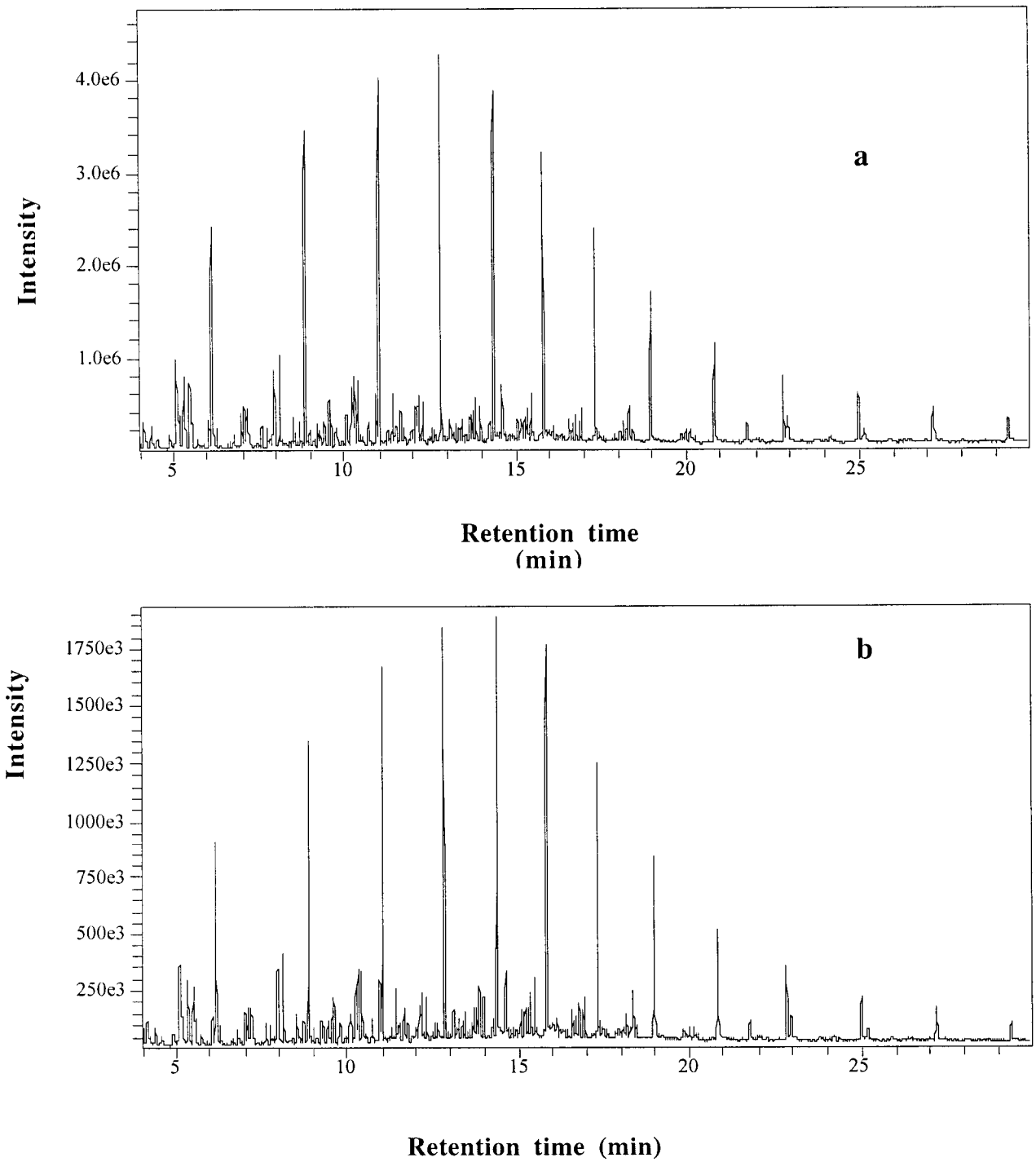

Figure 1.6 Total ion chromatograms of (**a**) untreated PA crude oil and (**b**) Pa crude after irradiated

Table 1.2 Qualitative analysis of untreated PA crude oil by total ion chromatography (TIC)

Retention Time (min)	Area (%)	Formula	MW	Compound
5.305	2.95	C_8H_{18}	114	3-Methyheptane
6.121	9.92	C_8H_{18}	114	Octane
7.925	3.13	C_9H_{20}	128	2,4-Dimethylheptane
8.086	6.26	C_8H_{10}	106	1,3-Dimethylbenzene
8.825	11.42	C_9H_{20}	128	Nonane
10.270	2.26	$C_{10}H_{22}$	142	2-Methylnonane
10.907	2.11	C_9H_{12}	120	1,2,4-Trimethylbenzene
10.992	11.81	$C_{11}H_{24}$	156	Undecane
12.805	12.35	$C_{11}H_{24}$	156	Undecane
14.401	10.81	$C_{11}H_{24}$	156	Undecane
15.853	9.22	$C_{11}H_{24}$	156	Undecane
17.315	7.37	$C_{14}H_{30}$	198	Tetradecane
18.958	6.06	$C_{14}H_{30}$	198	Tetradecane
20.800	4.33	$C_{14}H_{30}$	198	Tetradecane

Table 1.3 Qualitative analysis of residue from sonic treated PA crude oil by total ion chromatography (TIC)

Retention Time (min)	Area %	Formula	MW	Compound
6.139	10.02	C_8H_{18}	114	Octane
8.840	12.14	C_9H_{20}	128	Nonane
11.005	13.10	C_9H_{20}	128	Nonane
12.817	14.74	$C_{11}H_{24}$	156	Undecane
14.414	13.96	$C_{11}H_{24}$	156	Undecane
15.867	12.62	$C_{11}H_{24}$	156	Undecane
17.329	10.19	$C_{14}H_{30}$	198	Tetradecane
18.973	8.04	$C_{14}H_{30}$	198	Tetradecane
20.818	5.19	$C_{14}H_{30}$	198	Tetradecane

2.2.2 Development of the Numerical Framework

The equations governing the propagation of acoustic waves in a porous medium are non-homogeneous, nonlinear, hyperbolic equations resulting from the conservation of mass, energy, and momentum of each phase in the multiphase system. The equations of each phase are very similar and are distinguished primarily by the saturation of that phase in the porous medium. They are written in condensed form as shown in equation 2.1. The main focus in the development of this simulation model has been the solution of equation 2.1 given below.

$$\frac{\partial \vec{U}}{\partial t} + \nabla . \vec{F}(\vec{U}) = \vec{Q}(\vec{U}) \qquad 2.1$$

The first term of the equation describes the temporal variation in the conserved variable vector $\vec{U}$ representing the accumulation of these variables as they are transported through a physical domain. The physical domain is prescribed by appropriate definition of the grad operator $\nabla \cdot [\ ]$. Fluid transport is described by the flux vector, which is a function of the conserved variable $\vec{U}$. This makes the governing equations non-linear and adds to the difficulty of developing stable numerical algorithms for the solution of equation 2.1. Furthermore, the transport takes place in response to the source term vector $\vec{Q}(\vec{U})$. This vector is also a function of the conserved variables $\vec{U}$, which further complicates the numerical handling of this equation. In addition, the existence of these nonlinear forcing functions makes the equation non-homogeneous adding to the challenge of its solution.

Numerical solutions to this set of nonlinear, nonhomogeneous equations is notoriously difficult, especially in the presence of large discontinuities in the conserved transport variables, $\vec{U}$. Such discontinuities are always present when the fluids are subjected to strong pressure fluctuations resulting from the propagation of strong shock waves through the system, such as those generated by acoustic transducers. It was therefore determined that the first task was to develop numerical algorithms for the solution of this equation, simultaneously with the development of the governing equations. It should be noted that most formulations of the equations governing this type of fluid flow have similar left-hand-sides as will be seen in Section 2.2.4. However, differences

between simulating different phenomena are seen in the handling of the source terms, i.e. variations in the conserved variables $\check{U}$ occur primarily in response to the number of phenomena considered to be influential and are thus added to the source term vector $\dot{Q}(\check{U})$.

2.2.2.1 Solution Algorithms

No analytical solution exists for equation 2.1 and much of the focus has been in the development of an accurate numerical solutions. Most of the early research focused on developing accurate solutions for the pure advection problem, which is a subset of equation 2.1, obtained when the fluid transport is considered to occur in the absence of forcing functions. Such equations, referred to as Euler's equations, describe flow conditions that occur in response to discontinuities in the flow variables. Accurate numerical solutions to this set of homogeneous hyperbolic equations have been developed by eliminating the spurious oscillations and dampening that occurs at discontinuities that are present within the flow. The second-order accurate total variation diminishing (TVD) numerical scheme is an example of this work, and is incorporated in the model under development here. This numerical scheme produces high resolution of the discontinuities that exist in the flow, or those that may develop in response to forcing functions when the source term is considered.

When such source terms are considered, the numerical scheme is able to capture these discontinuities with very good resolution, however it is unable to accurately locate the shock in space. This is often a result of spurious solutions were the discontinuities travel at unphysical speeds. The severity of the inaccuracies resulting from the inclusion of the source term is dependent on the stiffness of the problem, which results from the incompatibility of the time scales of the homogenous and non-homogenous parts of the solution. This incompatibility occurs in the research problem under consideration where the modeling of the fluid dynamics of the multiphase mixture is governed by a system of equations where variations occur at a time scale proportional the speed of sound in the mixture. In contrast, the source terms are based on the thermodynamics of the flow whose time scale is infinitely small.

In recent years, research has focused on obtaining solutions to the stiff problem posed by this advection time scale versus source timescale problem. Although the problem of stiffness can often be handled by use of implicit formulations, this is not a feasible option due to the non-linearity of both the flux transport functions and those of the source

terms. This is further aggravated for multi-component flows where the temporal and spatial mesh sizes required to produce accurate results are prohibitive. For such flows, one option is the use of predictor-corrector schemes with a TVD constraint where an attempt is made to preserve some coupling between the advection problem and the source problem. Examples of this approach are the work of Le Veque and Yee (1990) and Roe (1986). Alternatively a time-splitting approach can be applied such that the different time scales of the advection/source problems are handled separately during an equal duration of time Δt. This approach is used in the model developed herein. In this approach the advantage is that the set of homogeneous equations is solved using a state-of-art numerical partial differential equation (PDE) solver such as the TVD scheme, in conjunction with a robust ordinary differential equation (ODE) solver for the source problem. This is achieved by the following algorithm, where the PDE is first solved as an initial-value problem where the values of the variables $\dot{U}^n$ at proceeding time-level are the input (i.e. the initial conditions, ICs).

$$\left.\begin{array}{l} \dfrac{\partial \dot{U}}{\partial t} + \dfrac{\partial \dot{F}(\dot{U})}{\partial x} = 0 \\ \text{with ICs } \dot{U}(x,t^n) = \dot{U}^n \end{array}\right\} \Rightarrow \dot{U}^{n+1}$$

This is followed by the solution of the ODE with the initial conditions given by $\dot{U}^{n+1}$ as follows.

$$\left.\begin{array}{l} \dfrac{d\dot{U}^{n+1}}{dt} = \dot{Q}(\dot{U}^{n+1}) \\ \text{with ICs } \dot{U}(x,t^n) = \dot{U}^{n+1} \end{array}\right\} \Rightarrow \dot{U}^{n+1}$$

In the model developed here, the TVD scheme is used for the PDE problem, while a fifth-order Runge-Kutta solver is used for the ODE problem. It should be noted the source terms may pose an ODE based on spatial variation, this can be handled as shown below, where again the ODE solver is the fifth order Runge-Kutta solver.

$$\left.\begin{aligned} \frac{dF(U^{n+1})}{dx} &= Q(U^{n+1}) \\ \text{with ICs } U(x,t^n) &= U^{n+1} \end{aligned}\right\} \Rightarrow U^{n+1}$$

In addition, the procedure can be modified to maintain the second-order accuracy of the TVD scheme as below. Here the source terms are first solved to update the solution to a time level of half the original duration Δt, followed by the PDE solution for the whole time Δt, then again followed by the ODE solution for the remain half of the time duration.

$$\left.\begin{aligned} \frac{dU^{n+1}}{dt} &= Q(U^{n+1}) \\ \text{with ICs } U(x,t^n) &= U^{n} \end{aligned}\right\} \Rightarrow U^{n+\frac{1}{2}}$$

$$\left.\begin{aligned} \frac{\partial U}{\partial t} + \frac{\partial F(U)}{\partial x} &= 0 \\ \text{with ICs } U(x,t^n) &= U^{n+\frac{1}{2}} \end{aligned}\right\} \Rightarrow U^{n+1}$$

$$\left.\begin{aligned} \frac{dU^{n+1}}{dt} &= Q(U^{n+1}) \\ \text{with ICs } U(x,t^n) &= U^{n+1} \end{aligned}\right\} \Rightarrow U^{n+1}$$

The source term in the model under development are actually a combination of terms, with the source terms for the phasial mass and energy balance equations being based on the thermodynamic time scale of equilibrium of the constituent fluids, while for the phasial momentum balance equations, they are based on the hydrodynamic time scale of the speed of sound in the mixture.

2.2.3 Code Validation

The standard benchmark for transient code validation is the sudden valve closure problem. In this test, a strong transient pulse is generated at the outlet by reducing the mass flux out of the computational domain to zero instantaneously, hence simulating sudden valve closure. In a two-phase flow environment, this generates two shock waves in the system that propagates back to the inlet, one in the gaseous phase and the other in the liquid phase. The aim of the test is to track the simulated backward propagation of the shock waves and compare their location and shape to those of the exact solution. On one hand, the aim is to compare physical aspects of the computed results based on the assumptions made in the formulation of the governing equations; while on the other hand, the aim is to verify that the numerical handling of the hyperbolic formulation does not lead to solution corruption.

The set of governing equations used in this test are those that describe the multiphasial environment in the pipelines and are based on Euler's inviscid representation of fluid transport. When the outlet value is suddenly closed, the fluid in the outlet block is forced to an abrupt halt as a result of the imposed boundary condition. Once that fluid stops, the fluid in the adjacent blocks should also follow the generation of a well defined strong shock wave that propagates backwards towards the inlet. Without the dissipative effects of viscous fluid flow, the shock waves should propagate as a sharp discontinuity; this physical property of the solution requires the computed output to have high resolution at the shock front. In addition, another physical outcome of the formulation is that the speed of the backward propagating (towards the pipe inlet) shock waves is known to be $v_g - c_g$ in the gas phase and $v_l - c_l$ in the liquid phase, hence the location of the shock can be predicted before hand.

The multiphase environment is set up as a flowing wet hydrocarbon gas, at a pressure and temperature such that the system is in the two-phase region of the gas's P-T diagram. This gas and its condensate are tied together both thermodynamically and hydrodynamically. The former is modeled by incorporating an equation of state to supply the hydrodynamic model with the fluids properties at the assumed vapor liquid equilibrium. This environment is chosen because of the simplicity of modifying the model for application to the governing equations of fluid transportation in the porous media.
In the numerical handling, the effects of numerical dispersion and dissipation in the computed solution must be minimized. This means that the computed solution must be free

of numerical oscillations at the shock front. In addition, the resolution of these fronts must be high, implying that numerical viscosity added by the numerical scheme to eliminate frontal oscillation is adequate and efficient. This is because excess numerical viscosity would dampen the solution at the front, contradicting the basic Eulerian nature of the governing equations. The computed response of the model to the sudden outlet valve closure is presented as Run #1, and results are given in the Figures 2.1-2.22 along with descriptions of the events shown in each of the figures. The data on the test section used for Run #1 are given in Table 2.1; the composition of the gas used is given in Table 2.2.

Table 2.1 Pipe Date for Run #1

Inlet Pressure	900 psia
Inlet Temperature	70°F
Gas Flow Rate	500 MMscf
Pipe Length	1 mile
Pipe Diameter	30 inches
Pipe Roughness	0.0008 ft
Ground Temperature	60°F
Heat Transfer Coefficient	1 Btu/hr-ft^3-°R

Table 2.2 Natural Gas Composition

Component	Molar fraction	Component	Molar fraction
N_2	0.0101	NC_4	0.0171
CO_2	0.0032	iC_5	0.0028
C_1	0.7557	NC_5	0.0031
C_2	0.1122	C_7	0.0041
C_3	0.0778	C_8	0.0033
iC_4	0.0078	C_9	0.0028

Figure 2.1 shows the gas mass flux profiles, with each representing the gas mass flux at a particular time. The first curve represents the steady state gas mass flux profile that

existed in the pipe at the instant before the outlet valve was closed, while each of the other curves represents times that are one-second apart, after valve closure. In Figure 2.1, the gas mass flux is seen to go to zero at the outlet block, however in subsequent blocks the gas is significantly retarded but does not come to a halt. At these locations the gas motion is a result of the continuous compression experienced by the gas. This can be seen in Figure 2.2 showing the pressure profiles along the pipe, which indicate the rise in the system pressure at those locations. In Figure 2.3, we see that the density of the gas is also increasing at those locations. Furthermore, the fraction of the pipe that is filled with gas, i.e. the gas holdup, is seen to decrease at these locations due to the reduction of space required to accommodate the compressed gas. This is seen in Figure 2.4 showing the gas holdup profiles during the transient shock propagation. Finally the conserved variable is also seen to increase in Figure 2.5, as the mass of gas per unit volume of the block is increasing. This variable is also proportional to the partial pressure of the gas, with the local square of the speed of sound in the gas being the constant of proportionality during a given time step. Therefore increases in this variable also indicate that the gas is being compressed.

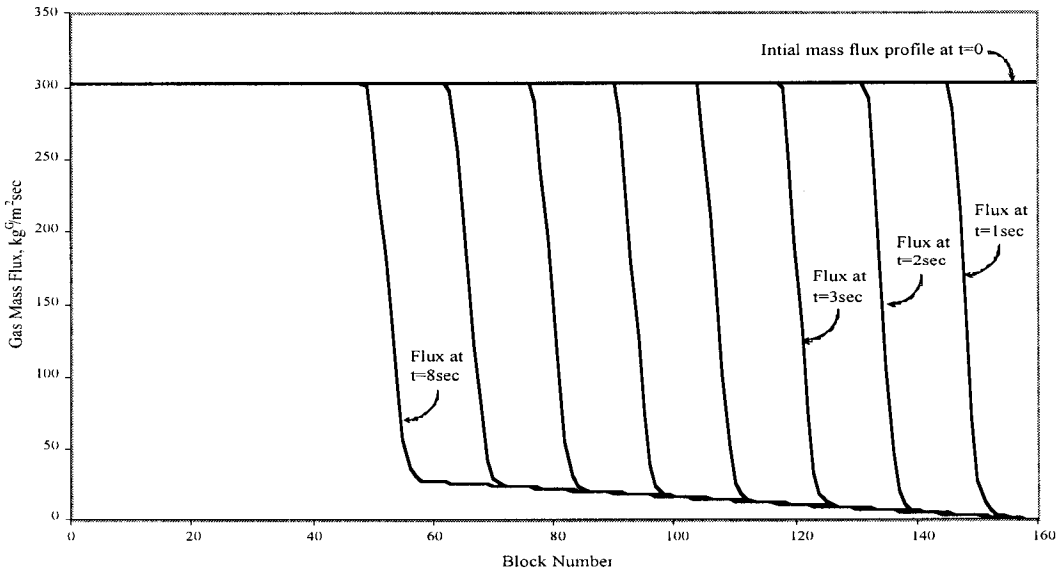

Figure 2.3 Gas mass flux after 8-seconds after sudden outlet valve closure

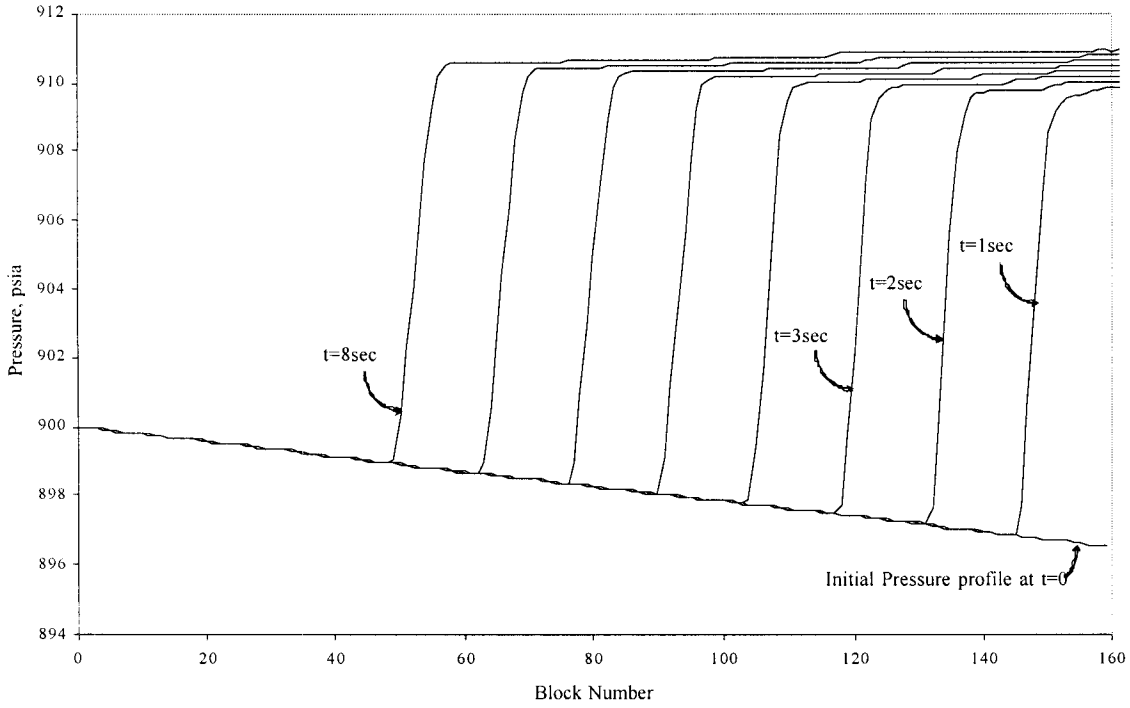

Figure 2.2 Pressure profiles after 8-seconds after sudden outlet valve closure

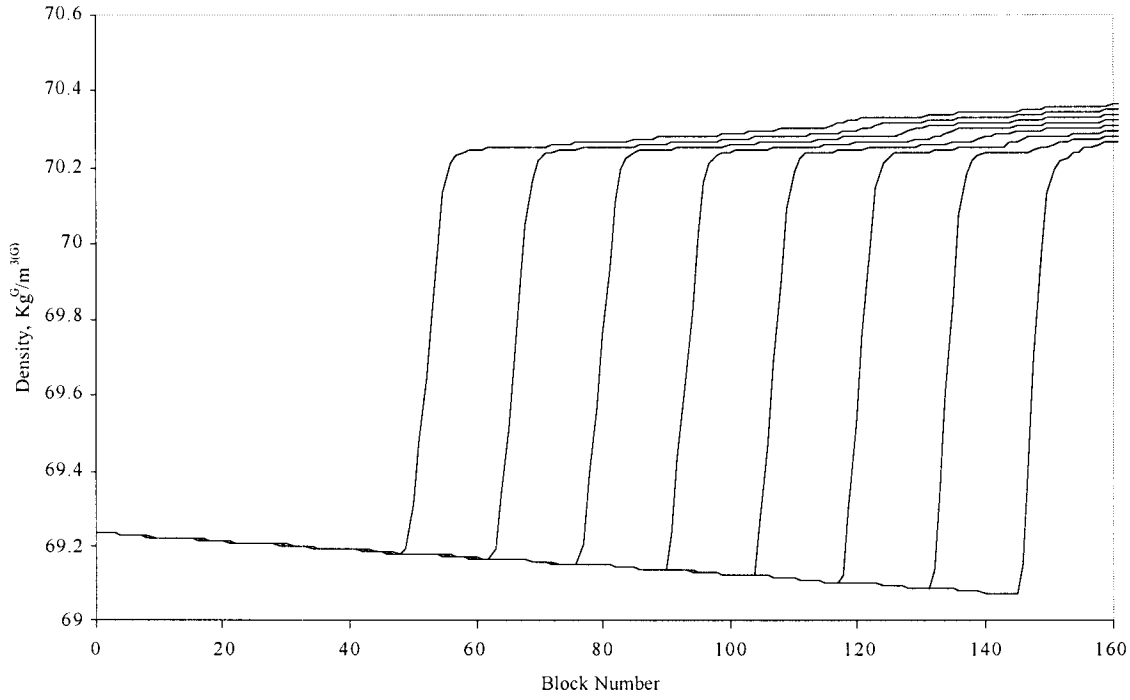

Figure 2.3 Gas density profiles after 8-seconds after sudden outlet valve closure

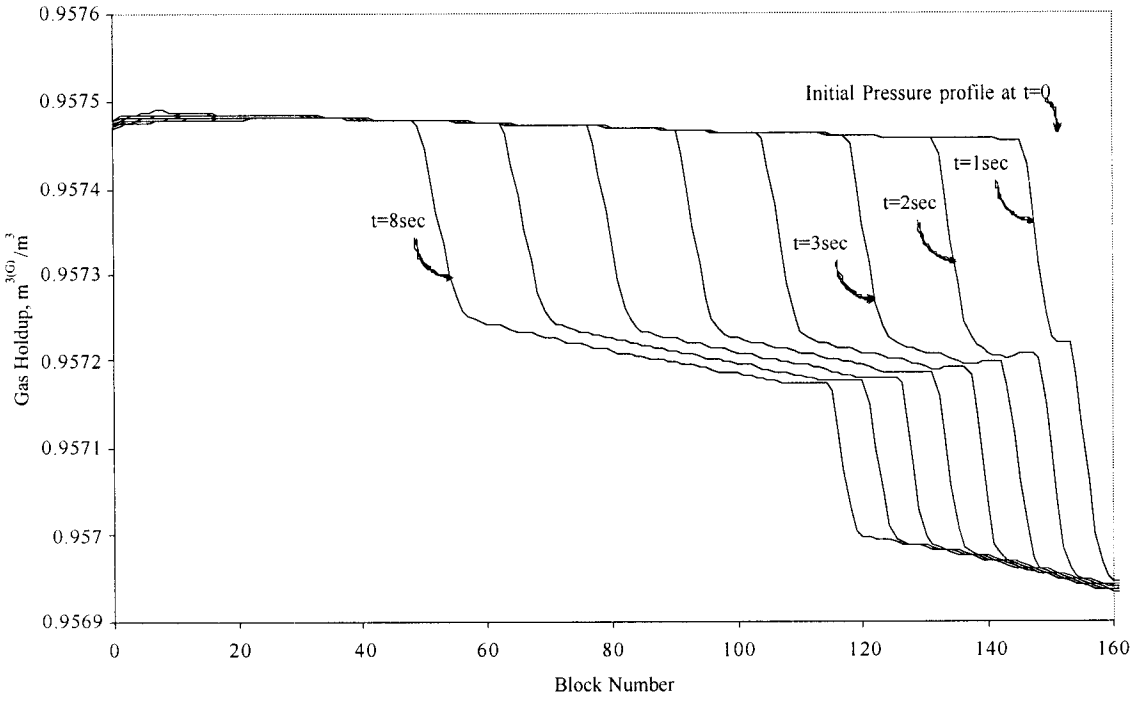

Figure 2.4 Gas holdup profiles after 8-seconds after sudden outlet valve closure

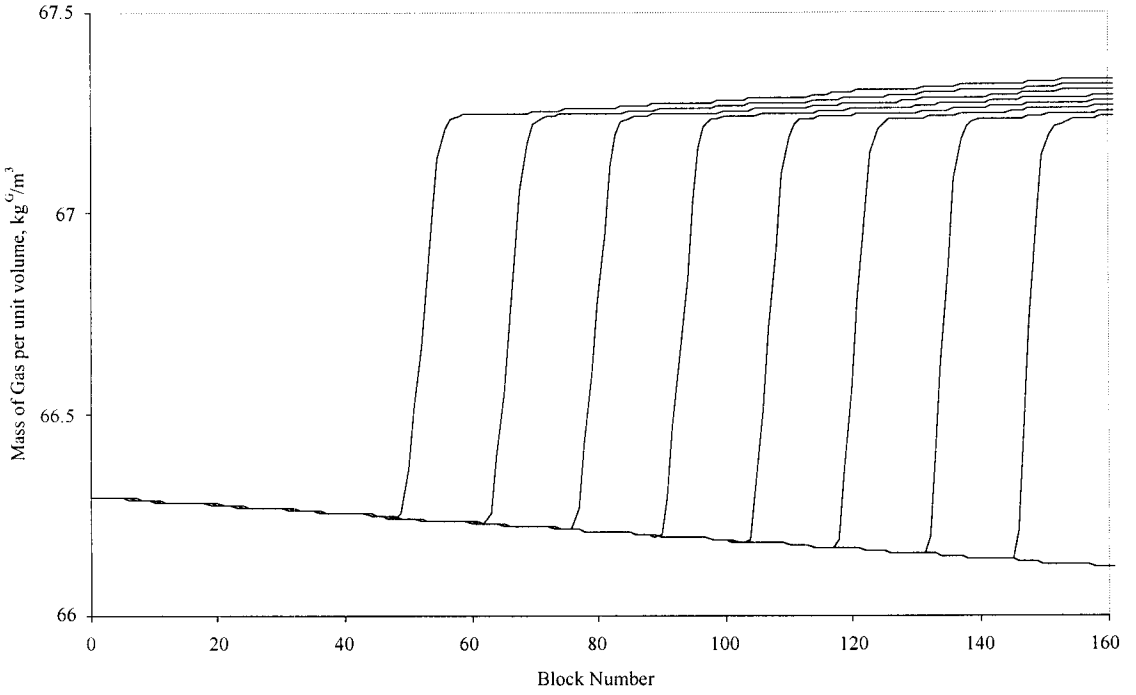

Figure 2.5 Mass of gas per unit volume profiles after 8-seconds after sudden outlet valve closure

Figure 2.3 suggests that there are two stages for this compression. This can be explained by the interphasial interaction that exists between the two phases as they compete for the cross-sectional area of the pipe. The figure shows the physical response due to the interaction between the phases as a result of the difference in the speed of propagation of the shock wave in each phase. As seen in Figure 2.1, the mass flux in the gas phase is dramatically reduced by the shock wave generated at the outlet due to valve closure. However, in the case of the liquid phase, the shock wave moves slower and due to the lower compressibility of the gas condensate, the liquid phase comes to a complete halt as a result of the sudden valve closure. This is seen in Figure 2.6, where the mass flux of the liquid phase shows the same two-stage response due to transient propagation of two shock waves. In the first stage, the liquid phase is brought to a halt due the shock in that phase. However, in the second stage the effect of the reduction of gas velocity (due the shock wave in that phase) is seen to partially reduce the mass flux in the liquid phase. At these locations, the momentum in the liquid phase allows it to remain in motion, despite the frictional retardation force at the pipe walls. Postulating that the momentum is the sole cause of liquid motion is justified by recalling that the liquid phase is made mobile primarily by the pull of the gas phase on the liquid phase at their interface. This is determined by the differential phasial velocities that lead to the development of the interfacial drag force. Once that is significantly reduced due to the retardation of the gas phase, only the liquid momentum keeps the liquid mobile at those locations where the shock propagating in the liquid phase has not arrived. On the contrary, at this location it is the liquid phase that is 'pulling' the gas phase, as shown in Figure 2.7. However this 'pull' does not cause an increased gas velocity but rather it aids in compression of the gas at those locations. It is clear that the second stage of gas compression occurs only when the liquid comes to a halt, leading to the competition for cross-sectional area of the pipe without the effects of the forces due to the mobility of the phases. At these locations, the much greater density and lower compressibility of the liquid phase mean that it will always prevail in increasing its share of the cross-sectional area of the pipe, as seen in Figure 2.8. This increased liquid fraction results in an increase in the mass of liquid per unit volume as seen in Figure 2.9. Finally, it is clear that the two-stage development of the shock propagation can be seen in all the properties of the liquid phase, since the faster moving gas phase shock affects all these properties. The gas phase only experiences the slower shock in the liquid phase as a result in increased compression due to the liquid coming to a halt, as seen in the its holdup volume fraction of Figure 2.3.

As a result of the shock propagation in the system, the local temperature is seen to increase due to Joule Thompson heating effect resulting from the increased local pressure. This causes an increase in the enthalpy carried by each phase, as is seen in Figures 2.10 for the gas phase and Figure 2.11 for the liquid phase. The combined effect of this increase in enthalpy is in the increase in the local temperature as seen in Figure 2.12. Finally, as a result of the increased local pressure and temperature of the system, the liquid phase is observed to undergo a slight expansion as seen in the small reduction in the phasial density of the liquid in Figure 2.13.

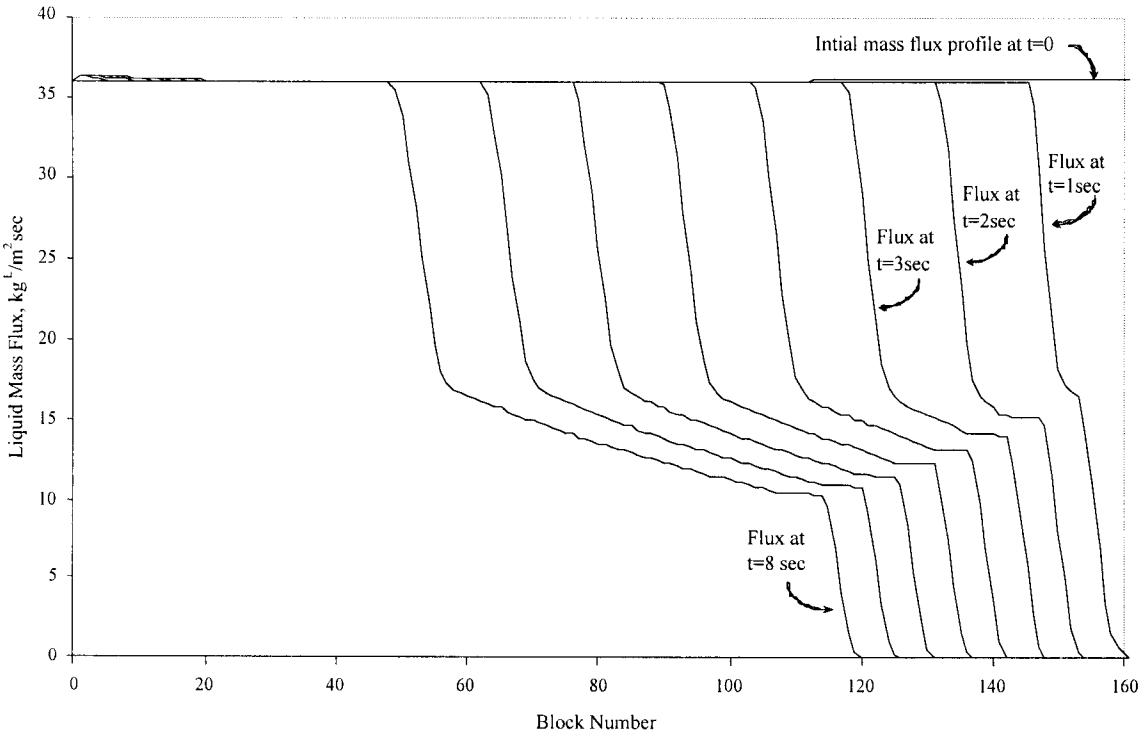

Figure2.6 1 Liquid mass flux after 8-seconds after sudden outlet valve closure

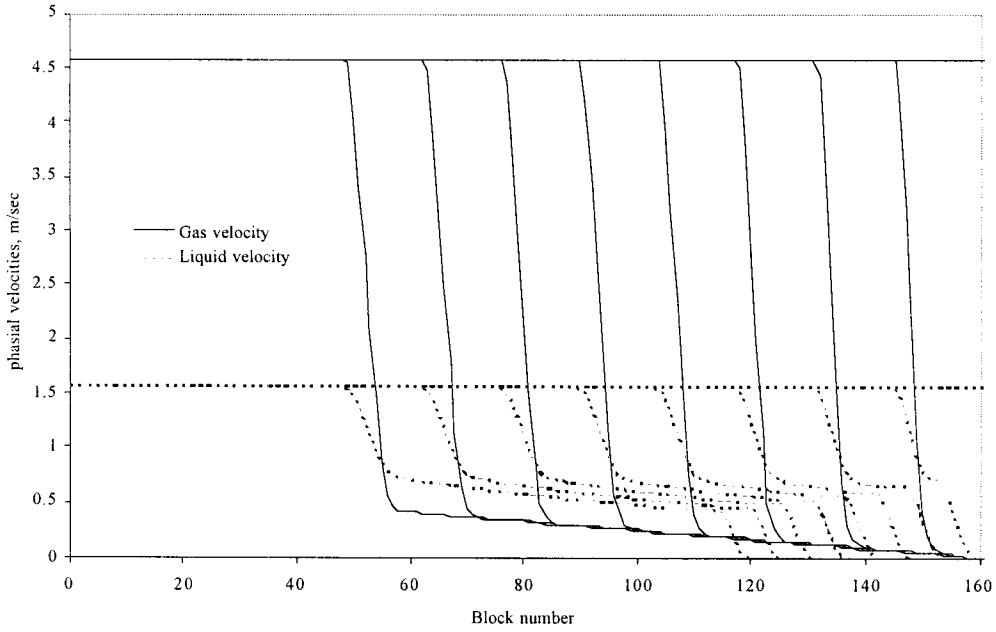

Figure 2.7 Phasial velocity profile after 8 seconds of shock propagation.

At this stage, the ability of the numerical model to predict the hydrodynamic behavior of the two-phase system has been established. The next objective of the code validation test is to show that the numerical schemes are able to alleviate the difficulties associated with the hyperbolic nature of these equations and their associated source terms. It is clear from the figures that the problem associated with numerical dispersion at the shock fronts is not seen in the results. However, in the following discussion, the steps taken to obtain the increased resolution of Figures 2.1 to 2.13 are described.

The resolution of shock at the discontinuities shown in the preceding figures can be quantitatively compared to the exact solution by the use of x-t diagrams similar to those in Figures 2.14 and 2.15. However, it should be noted that since the exact solution is not known due to the non-linearity of the problem, the x-t diagrams in Figures 2.14 and 2.15 are presented without the exact solution, but are still useful in comparing the resolution of different solutions. It is obvious that the best frontal resolution occurs when the distance between the front and back ends of the discontinuity is minimal, and is not increasing. This resolution is known to be affected by the flux limiting algorithm implemented as well as the Courant-Friedrichs-Lewy (CFL) number used. Two flux limiters are implemented to achieve the high resolution desired from the second-order TVD schemes; these are the Superbee and Minmod algorithms.

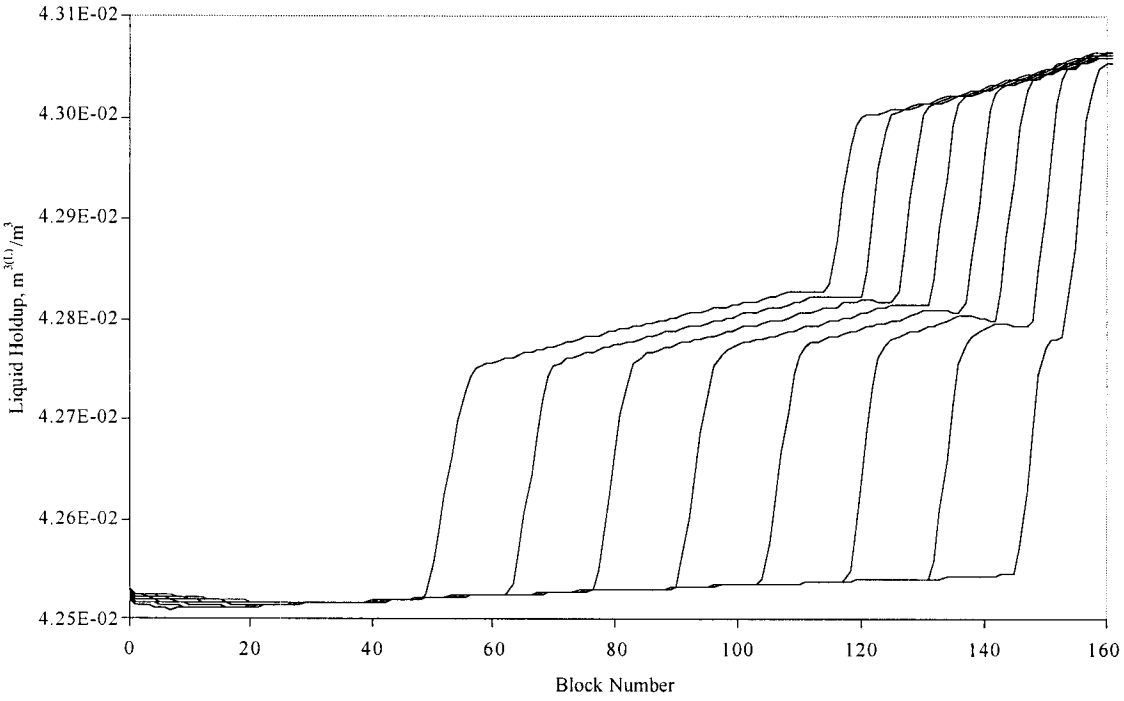

Figure 2.8 3 Liquid holdup profiles after 8-seconds after sudden outlet valve closure

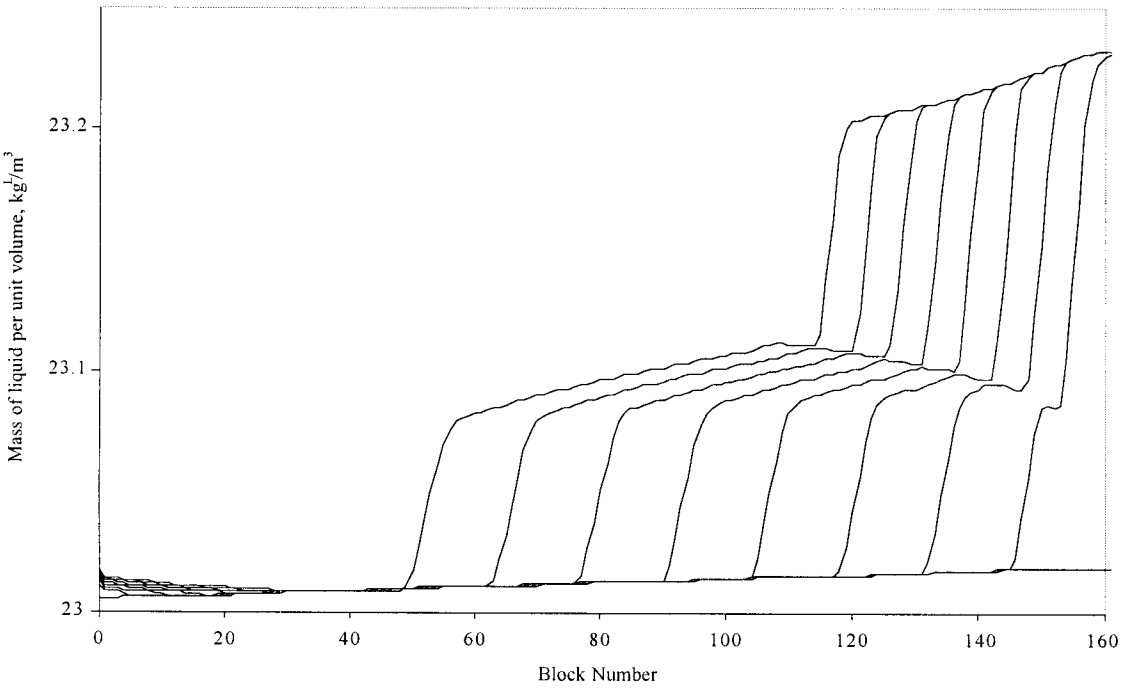

Figure 5.24 Mass of liquid per unit volume profiles after 8-seconds after sudden outlet valve closure

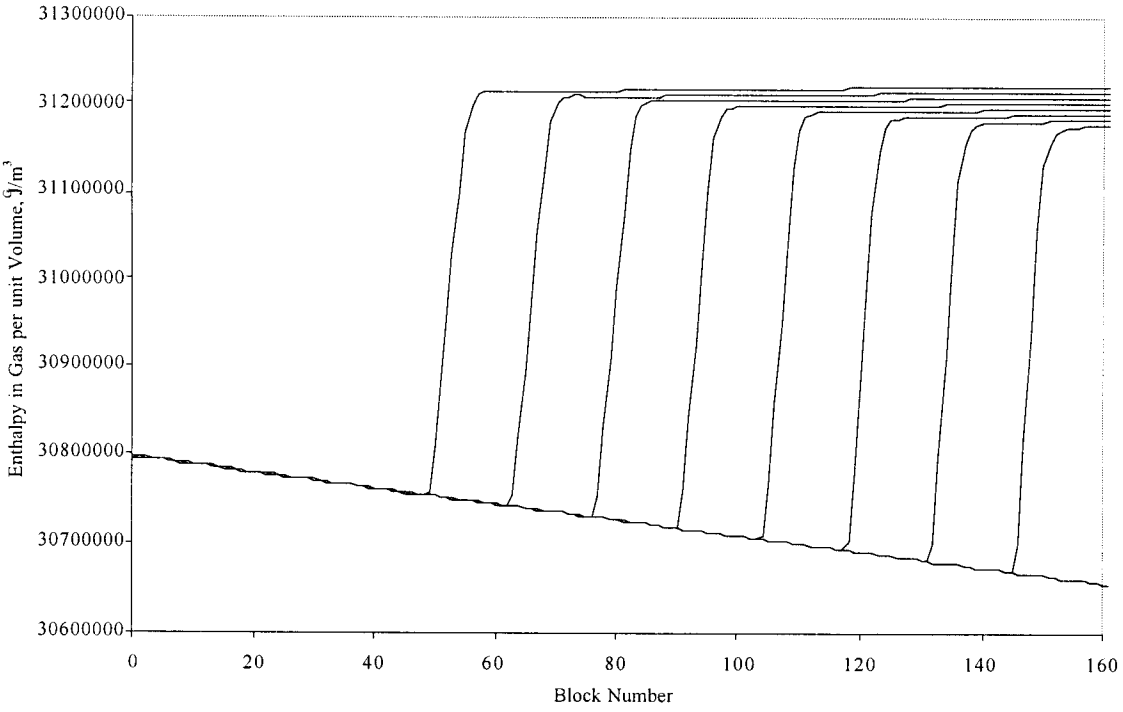

Figure 2.10Enthalphy in gas per unit volume profiles after 8-seconds after sudden outlet valve closure

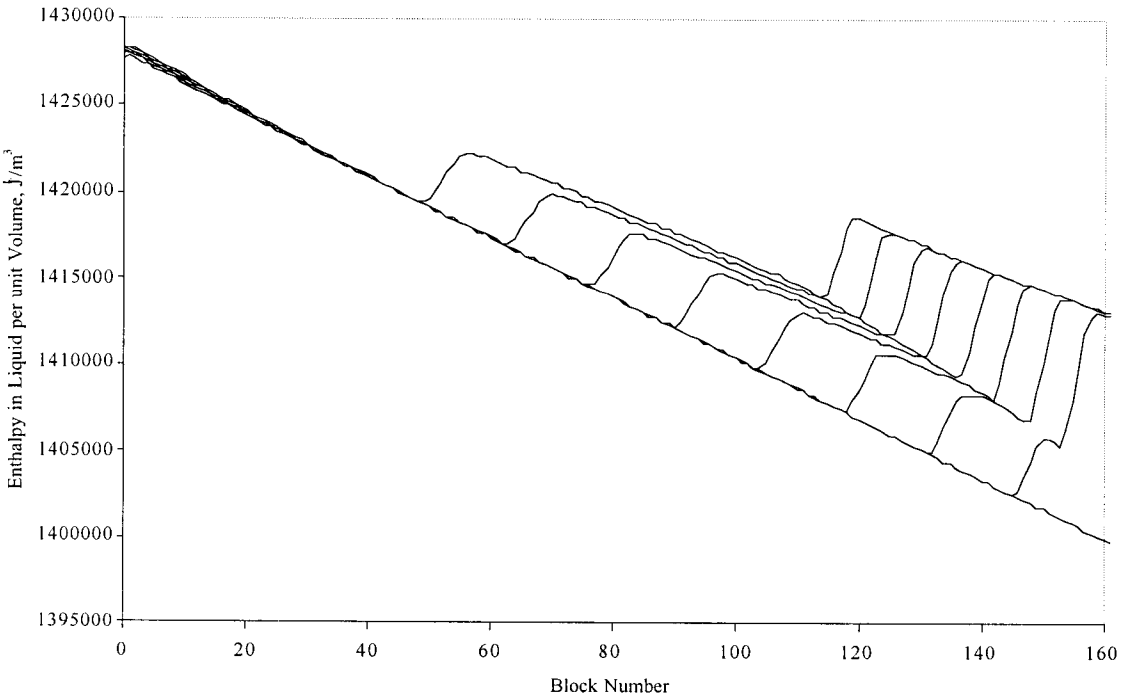

Figure 2.11Enthalpy in liquid per unit volume profiles after 8-seconds after sudden outlet valve closure

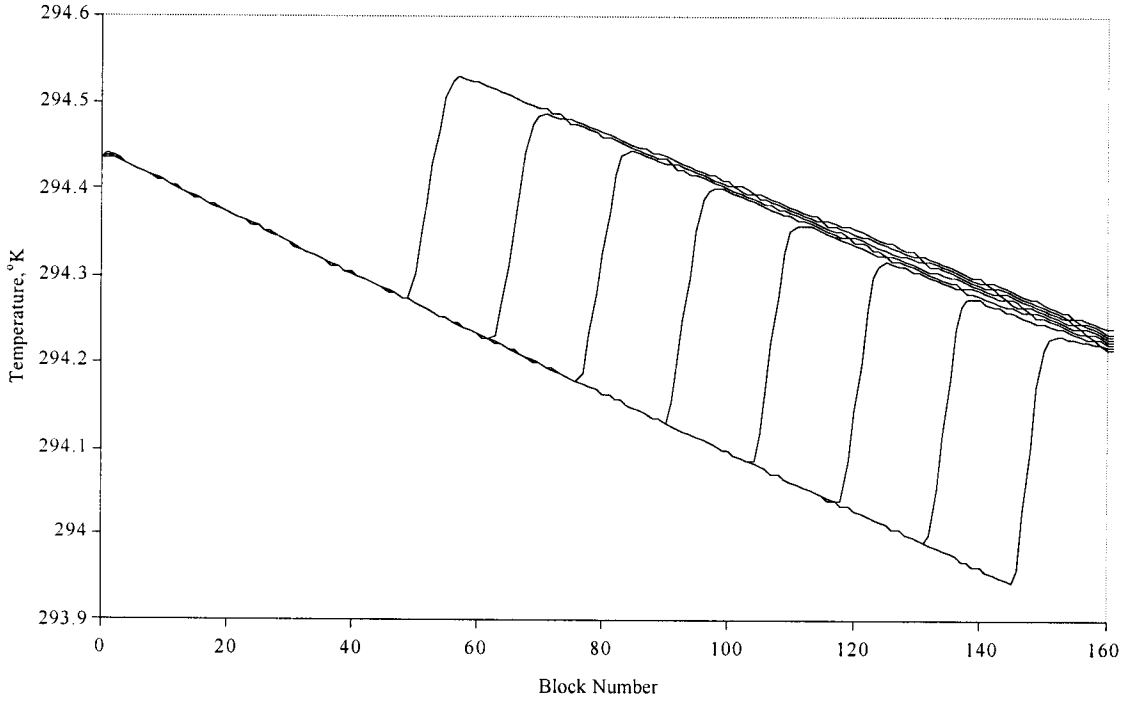

Figure 2.12 Temperature profiles after 8-seconds after sudden outlet valve closure

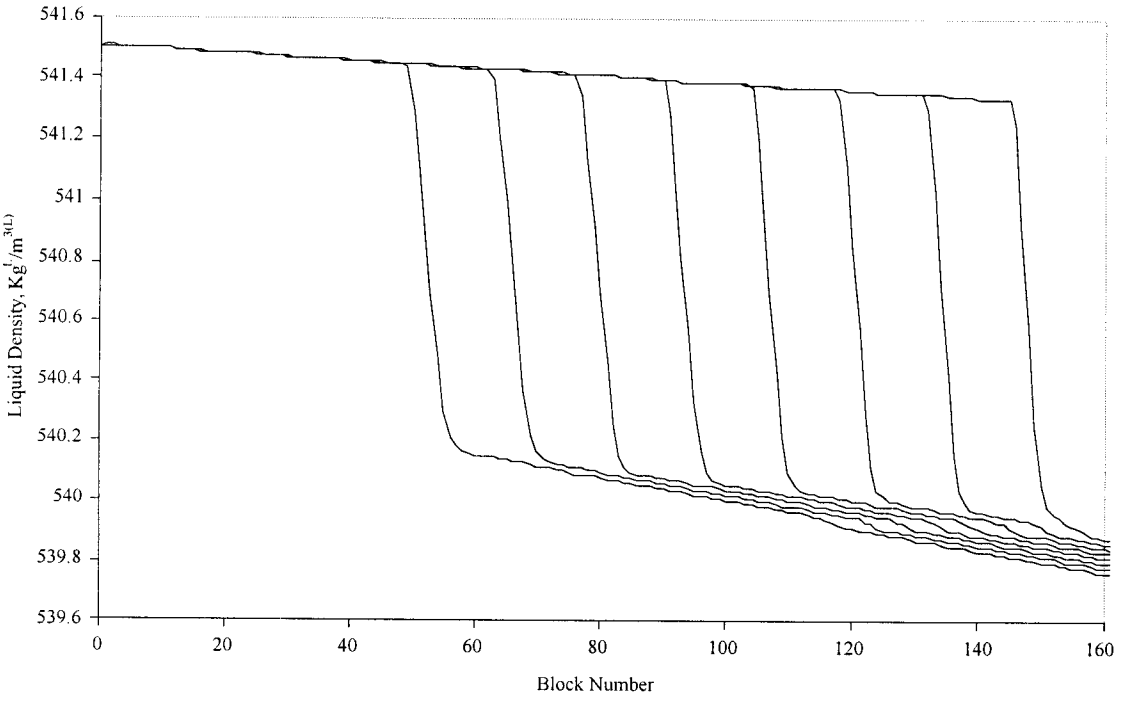

Figure 2.13 Liquid density profiles after 8-seconds after sudden outlet valve closure

The importance of the CFL number for resolution of the discontinuities is discussed. It is used to set a limit on the time step in the computation to ensure that the discontinuity does not enter **and** leave a block within the same time step. If this were to occur, the location of the discontinuity could not be accounted for during that time step. It is clear that this is done by accurate knowledge of the speed of propagation of the front at all blocks. The speeds of shock propagation is known to be given by the eigenvalues of the matrix $\dot{U}$, which is the derivative of the Flux vector $\frac{\partial \dot{F}(\dot{U})}{\partial U}$ with respect to the conserved variables vector$\dot{U}$, and is given by the systems governing equations, hence it is not under the control of the user to choose the desired time step. However the size of the block can be chosen to obtain different durations for the time step used. Larger block sizes would lead to larger time step sizes, with the price being a loss in the accurate representation of the physical domain, as a result of averaging over greater block sizes. On the other hand, accurate representation of the system properties by decreased block size leads to a greater requirement of CPU time, leading to longer run times. Finally, if the user has decided on a maximum acceptable block size, then varying the value of CFL number can be shown to cause variations in the resolution of the shock front.

To test of the shock front resolution achievable under different CFL numbers and with a predetermined block sizes, several runs were carried out using CFL numbers of 0.04, 0.16, 0.32, 0.64, and 0.96. Furthermore, in order to test the performance of each of the flux limiters, the runs where repeated twice, once using the Minmod limiter then using the Superbee limiter. In Figure 2.14, the results obtained for the five CFL numbers using the Minmod limiter are presented. Figure 2.15 shows the results obtained using the same CFL numbers while implementing the Superbee flux limiter. From the results shown, the Superbee Flux limiter is seen to outperform the Minmod limiter; this is determined by the divergence of the lines showing the location of the front end of the shock wave and that showing the backend of the wave. Diverging lines imply that the front is smeared by the addition of excessive numerical viscosity to control the frontal oscillations. In both figures, the lines are seen to be diverging; however, as the CFL is decreased the divergence in the Superbee case is seen to decrease. This is especially true for the lowest CFL number, where in the Superbee case there is no realizable divergence, hence no realizable deterioration of the resolution of the shock with respect to time.

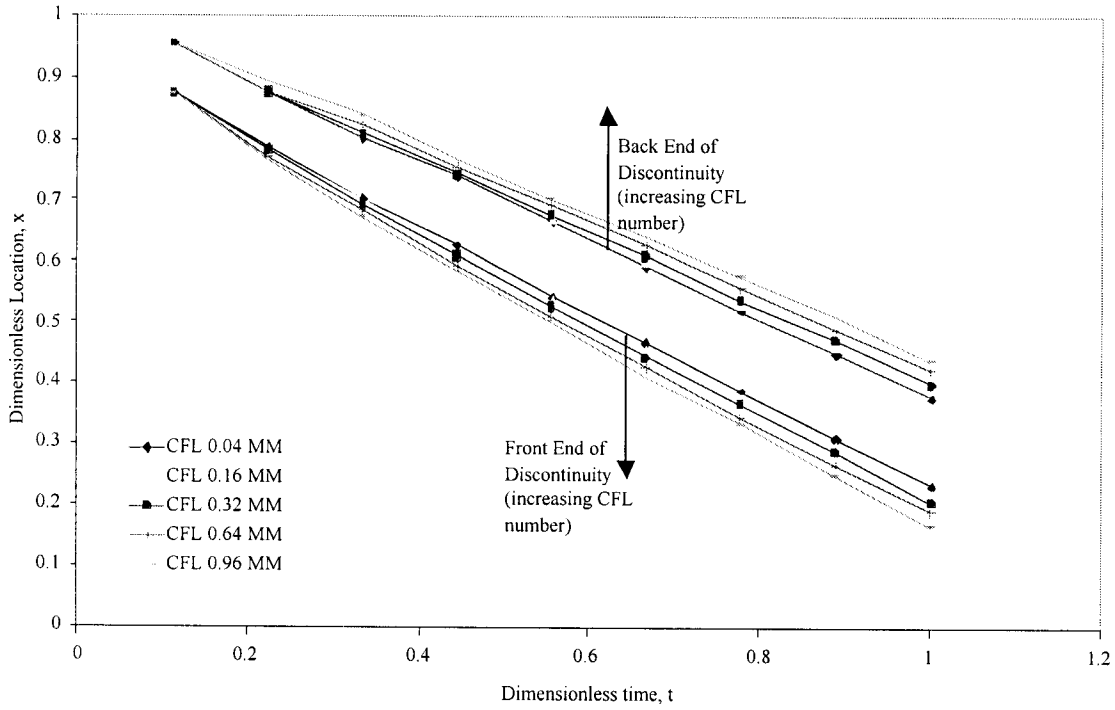

Figure 2.14Minmod x-t diagram showing that the shock resolution is progressively deteriorating

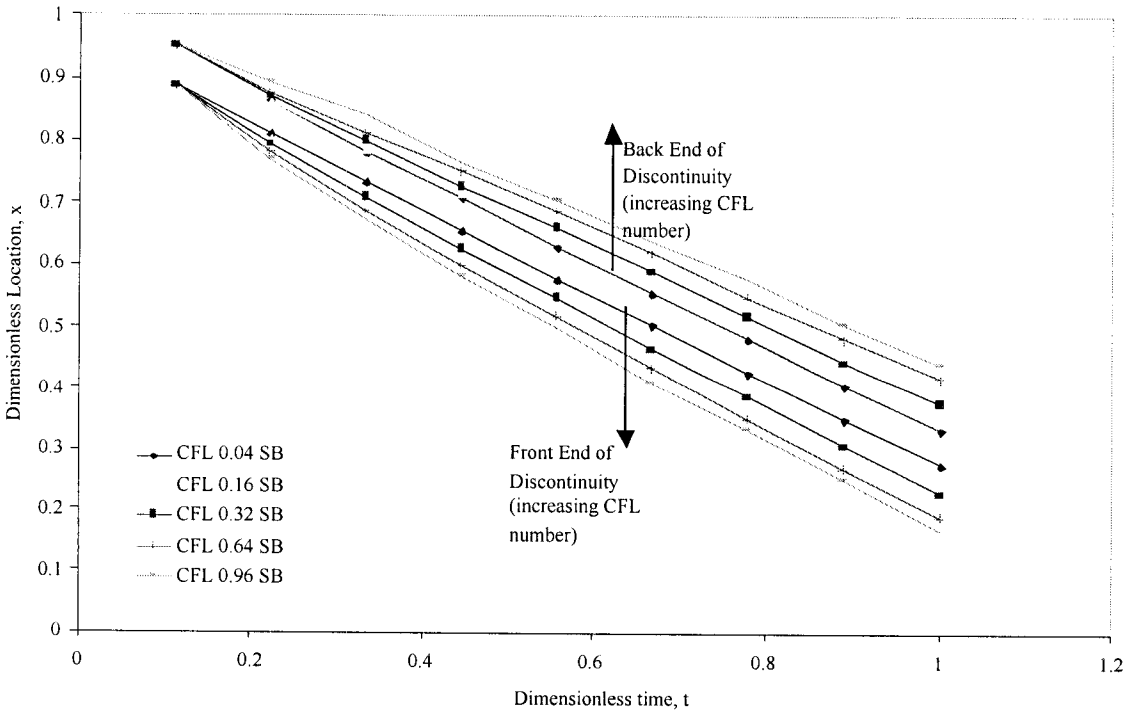

Figure 2.15 Superbee x-t diagram showing that the shock resolution is progressively deteriorating

The pressure profiles using the Minmod flux and Superbee flux limiters at the various CFL numbers are shown in Figures 2.16 and 2.17, respectively. It is clear that the performance of both limiters improve at lower CFL numbers. However the Superbee limiter again outperforms the Minmod limiter, since the improvement in the resolution is more dramatic. The results shown for the pressure profiles are representative of all the other system's properties. It should be noted that the results shown in Figures 2.1 to 2.13 are obtained using the Superbee limiter with the CFL number set at 0.04.

It is clear that at low CFL numbers the Superbee limiter outperforms the Minmod limiter; however, at higher CFL numbers their performance is similar. As a result, Superbee is chosen as the primary limiter for all future runs, since improvement in the shock resolution is always achieved with no extra computational overhead. However, the choice of the best CFL number for the future runs is less obvious since the difference of computational overhead between CFL number 0.96 and 0.04 is huge. This is clear since the time step in the 0.96 case is 16 times larger than that in the 0.04 case. In choosing the appropriate CFL number to use, the important issue is the significance of the location of the shock front. If that location is essential to the objective of the simulation, then a low CFL number should be used.

The primary objective of this study is the propagation of sonic pulses through a porous medium. Furthermore it is noted that in such a medium wave propagation is subjected to significant diffusion due to the importance of the second order terms. Therefore, although the accurate location of wave front is important for locating physical phenomena associated with it, it may be smeared due to the effect of physical diffusion as opposed to artificial numerical diffusion. As a result a relaxed CFL number may be used, a subject to review once the development is complete.

2.3 Task 3. Development of a New Generation of Acoustic Transducers

2.3.1 Introduction

Transducers, projectors and rarely hydrophones, are the primary components of acoustic-enhanced fluid-flow and near-wellbore damage experiments. Projectors are often obtained from vendors for the generation of pressure waves in liquids. Users are often limited by the manufacturers technical specifications and are therefore forced to operate within available settings. Consequently, systematic investigations of flow-enhanced parameters are poorly defined and irreproducible. As an example, Gollapudi et al., used an ultrasonic method for the removal of asphaltene deposits during petroleum production. They did not specify the brand or model of the commercial ultrasonic transducer (distruptor

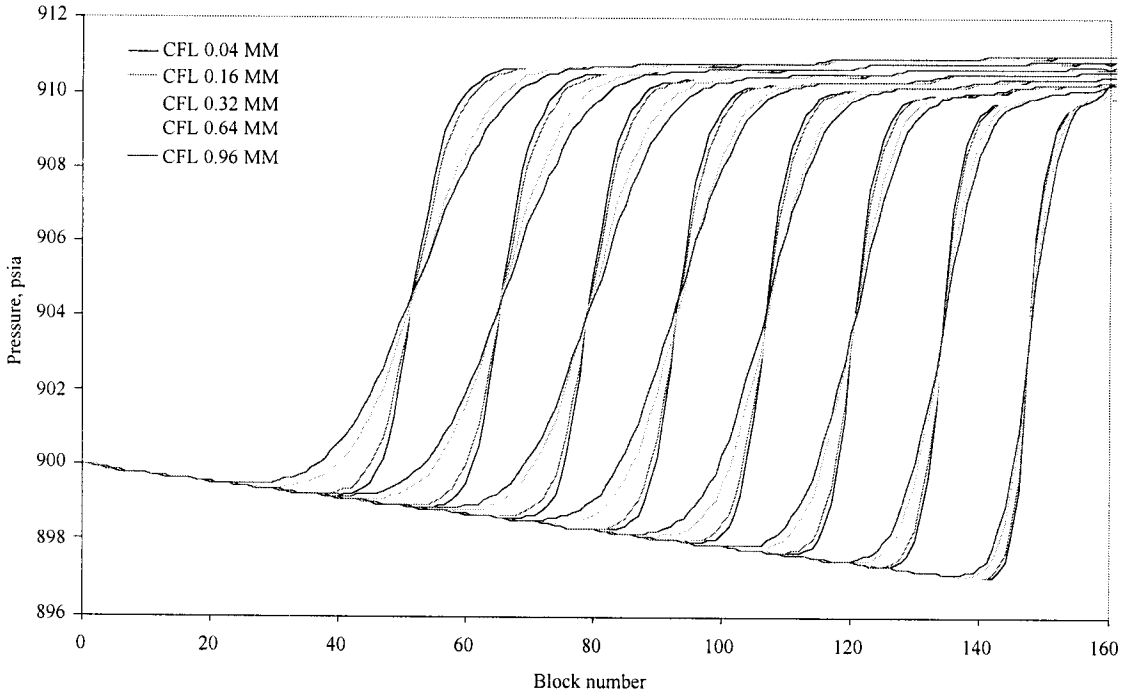

Figure 52.16Comparisons for pressure profiles after 8-seconds after sudden outlet valve closure, using the Minmod flux limiter and a variety of CFL numbers

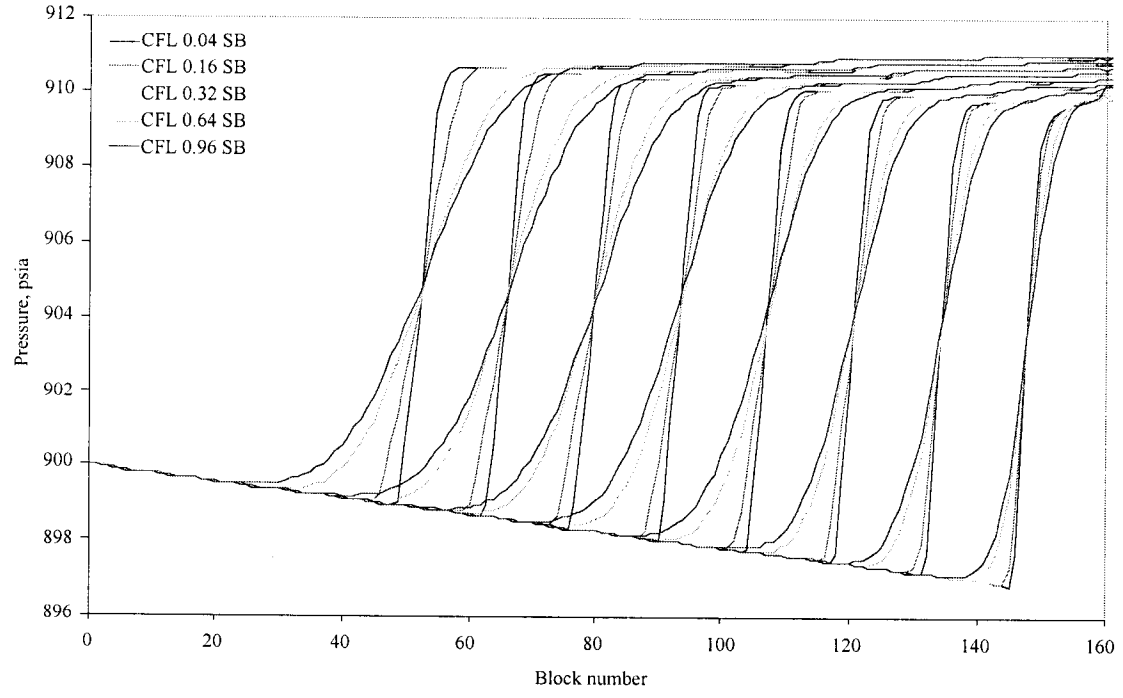

Figure 52.17Comparisons for pressure profiles after 8-seconds after sudden outlet valve closure, using the Superbee flux limiter and a variety of CFL numbers

horn) used. In addition, the output values were stated in the form of the output control settings, but not in terms of power (watts) or acoustic intensity. The reproducibility of such an experiment may be difficult, if not impossible, due to insufficient information. The need to understand the governing mechanisms of acoustic energy-fluid–solid interactions in porous media requires versatile transducers that can be operated within various parameters. Transducers were supplied by ARL to carry out basic experiments at room temperature and pressure in order to shed some light on the acoustic energy-fluid interactions in porous media.

2.3.2 Transducers and Hydrophone Calibration

Three piezoelectric projectors, two 20 kHz and one 40 kHz were supplied for laboratory-scale experiments. They are "low Q" transducers, which allows them to be used for a short pulse of ultrasound consisting of a broad range bandwith of frequencies. One projector has a square radiating head with a total area of 12.25 cm^2. The other transducer's radiating face was ground to a circular form with a reduced area of 9.62 cm^2, for easy coupling into the test apparatus (Figure 3.1). The 40 kHz circular projector has a radiating face of total area 7.07 cm^2. Two Polyvinylidene Fluoride (PVDF) hydrophones embedded in polyrethane, one circular (5.07 cm^2) and the other rectangular (6.45.0 cm^2) were supplied by ARL. The circular hydrophone was calibrated in the ARL fresh-water pool, assuming the speed of sound to be 1,480 m/second and density 1,000 kg/m^3. The hydrophone receive response is calculated from measurements of the source transducer and hydrophone voltage waveforms. Free field voltage sensitivity (FFVS) or the receive sensitivity is typically defined as dB relative to 1 volt per micropascal input (Figure 3.2). The figure shows measurements taken with and without lead urethane acoustic backing as a function of frequency.

2.3.3 Determination of Resonance Frequency of a Branson Horn

The resonance frequency of a Branson transducer was determined at ARL in order to be able to operate it in non-cavitation and cavitation regimes, using equipment listed in Section 2.1.4. The transducer's accompanied factory power converter and power supply (model 250) are designed to energize the transducer to the cavitation level regardless of the duty cycle, mode of operation (pulse/continuous wave) and/or output control setting. This particular transducer is considered to be a "high Q" transducer. It responds to a short voltage pulse with a relatively long lasting vibration decay time, emitting ultrasound with a narrow bandwidth. The resonance frequency was determined to be 24 kHz.

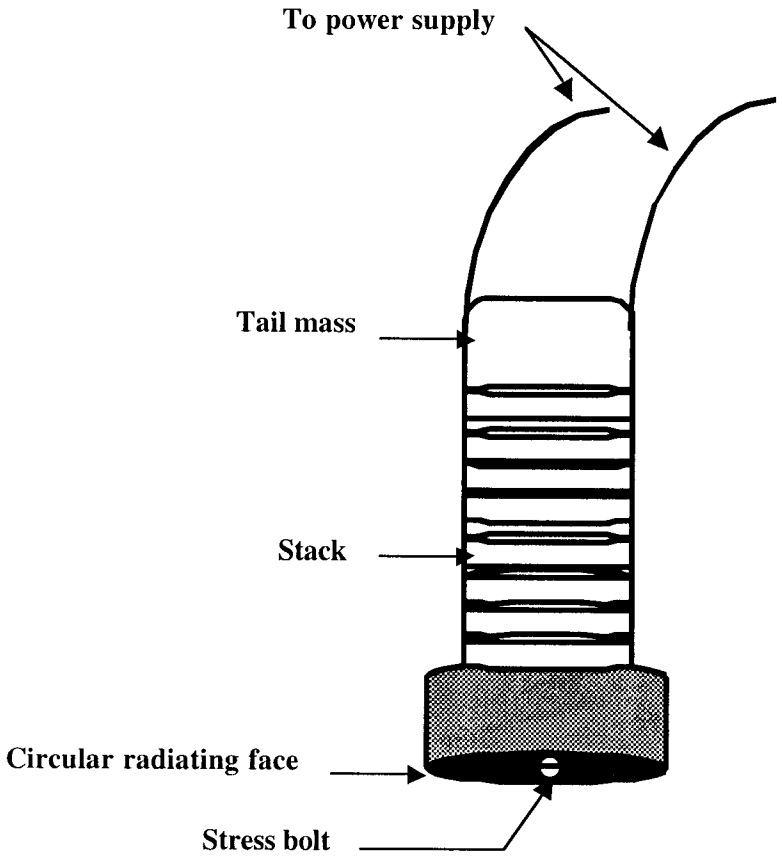

Figure 3.1 A circular Tonpilz or Longitudinal Vibrator

2.4 Task 4. Field Testing of the Sonication Technology

The overall plan for Task 4 is to perform field trials of the sonic transducer design. These trials will take place in production and/or injection wells located in Pennsylvania, New York, andWest Virginia. The field trials are expected to require three months of preparation time and one year of testing time.

2.4.1 Year 1 Work

Work performed during the first year included the start of several tasks leading towards the actual field testing of the sonication equipment. Examples of these tasks are literature searches, meetings with producers, information and sample gathering, and drilling four new wells for project use.

A literature search and review of four targeted production formations was initiated. Production from the Glade, Clarendon, and Gordon formations has occurred for over 100 years. Due to this length of time, the most recent information found on these formations

was from the mid 1960's. The bulk of the Bass Islands production is more recent and the literature dates to the early 1990's. Copies of this information can be found in Appendix B.

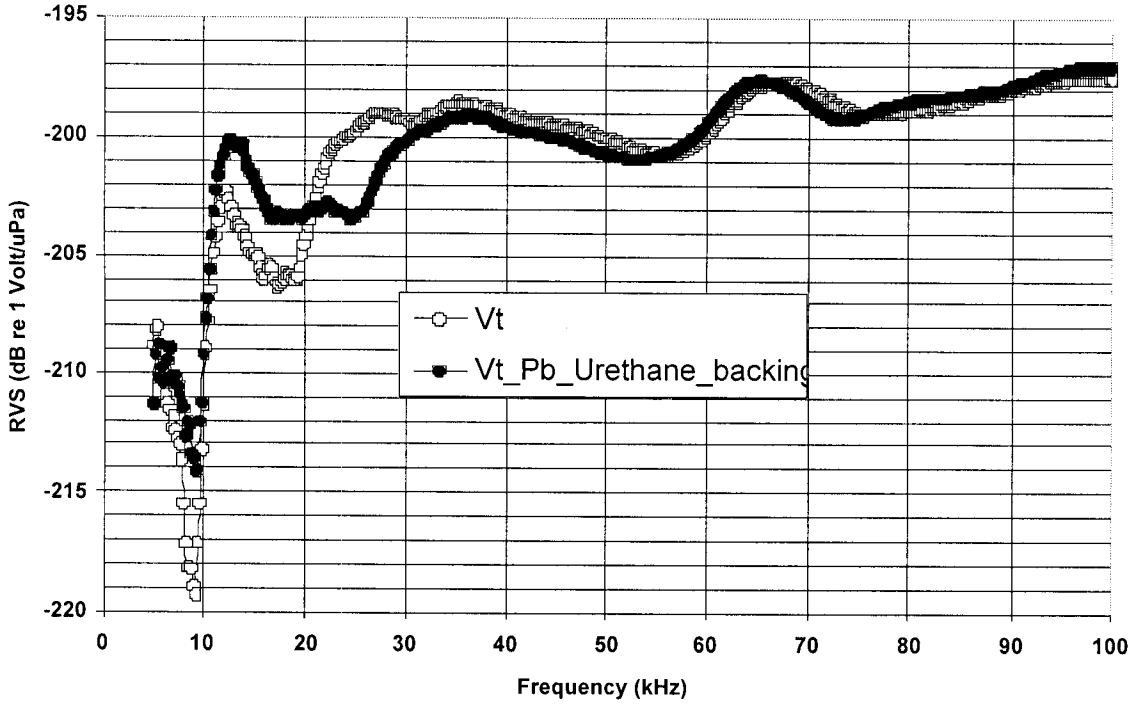

Figure 3.2. Receive voltage sensitivity (RVS) as a function of frequency for the Applied Research Laboratory (ARL) hydrophone 1/4 inch 1-3 composite, 1 inch diameter

Other work includes meeting with four independent oil producers to organize plans for the project. Plans varied for each operator, depending on the quantity and types of wells to be used in the project. This work is described in the subtasks listed below.

2.4.2 Evaluation in Partially Depleted Sandstone

The operators involved in this subtask are I.L. Geer and Sons (ILG) and Metzgar Oil Company (MOC). Located near Warren, Pennsylvania, both operators produce oil, water, and gas from either the Glade formation or a combination of Glade/Clarendon formations. ILG has drilled four new wells for the project while MOC has contributed an older production well.

ILG drilled and completed four wells during fall 2002 in the Glade Field. This field is located near Warren, Pennsylvania and has been producing for over 100 years. The four new wells penetrate the Glade, Clarendon and Balltown formations. Similar to most wells in this region, the completion method is openhole style. Figure 4.1 shows a typical completion for the ILG wells. Next, the wells were logged using Schlumberger's Air-Quad logging suite of Gamma-ray, Litho-Density, Compensated Neutron, Array Induction, Temperature and Caliper logs. This suite was used because it provided excellent resolution, calculated porosities and calculated water saturations. Figure 4.2 shows a of the Glade sandstone log. After air-notching the sandface at multiple depths, the wells were hydraulically fractured using a mixture of water, sand and additives. Following cleanup, the wells were piped into service with a beam pumping unit for lifting liquids and a gas meter to measure natural gas production. A separate 100 barrel tank was set for each well. Figure 4.3 shows the equipment arrangement for a typical well.

Production from three of the four wells has changed from mostly fracturing fluids to a mixture of oil, water, and natural gas. Production amounts are recorded to establish a baseline. This baseline will be used to determine the success of the sonication equipment. Problems with the fourth well have prevented any hydrocarbon recovery. These problems are being worked on and hopefully this well will stop producing fresh water.

The MOC well penetrates the Glade and Clarendon formations. This well has produced for many years. Pumped once per week, this well produces around three-quarters of a barrel of oil per week along with some water and natural gas. Original well and production records have not been located. Plans are underway to search several sources.

We have received oil, production water, paraffin and fracturing sand samples from ILG for laboratory testing. Our plans for these wells are to monitor the oil, water and natural gas production to establish a baseline. Finally, we will test the sonication equipment in these wells for approximately one year.

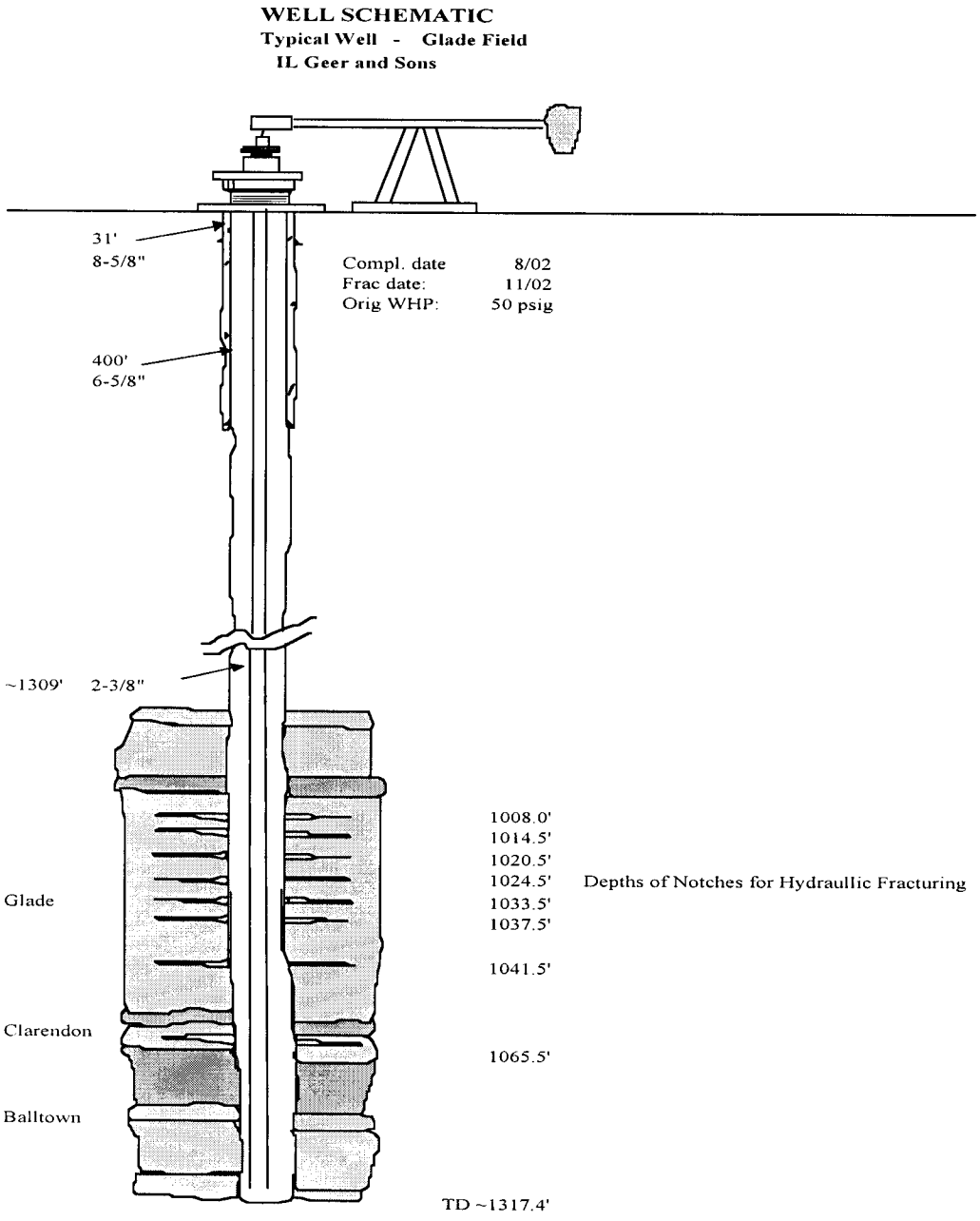

Figure 4.1 Schematic diagram of a typical completion for the ILG wells

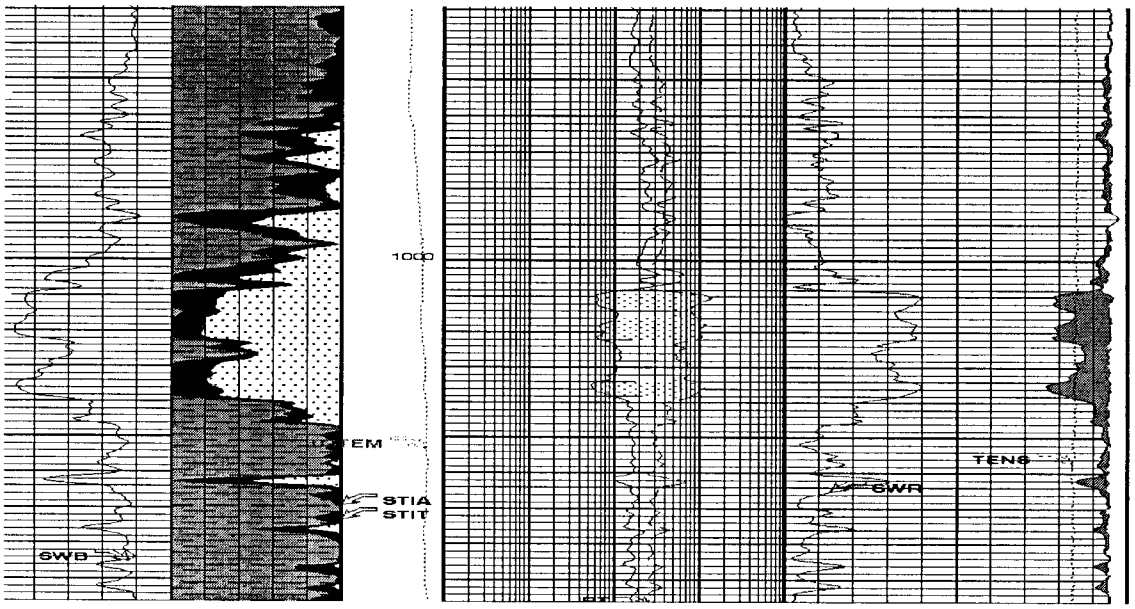

Figure 4.2 Section of the Glade Sandstone log

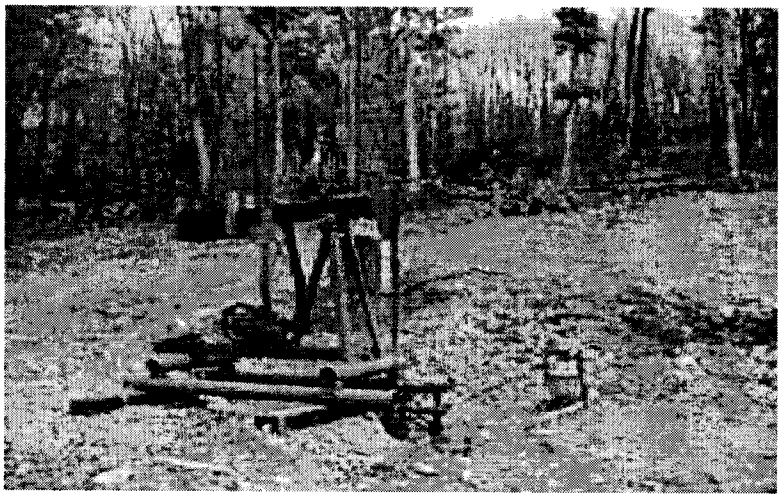

Figure 4.3 Equipment arrangement for a typical well

2.4.3 Evaluation in a Shot Hole

Our plan for evaluating the sonication equipment in a shot hole is to request the use of one or more wells from ILG near Warren, Pennsylvania. After choosing the

candidate(s), we will prepare measurement equipment to monitor the oil, water and natural gas production. Production should be measured for at least three months to establish a baseline. Finally, we will test the equipment in their well(s) for about one year.

2.4.4 Evaluation in a Hydro-fractured Wellbore

Our plan for evaluating the sonication equipment in a hydro-fractured wellbore is to request the use of one or more wells from ILG near Warren, Pennsylvania. After choosing the candidate(s), we will prepare measurement equipment to monitor the oil, water, and natural gas production. Production should be measured for at least three months to establish a baseline. Finally, we will test the equipment in their well(s) for around one year.

2.4.5 Evaluation in a Fractured Carbonate

Lenape Resources (LR) is the operator involved in this subtask of the project. Located in Botavia, New York, LR produces oil, water, and natural gas from the Bass Islands. Bass Islands is a term used by drillers in the area when referring to the Akron-Bertie group of New York. Presently, LR has one candidate well with electricity access. This well, located near Jamestown, New York, produces a substantial amount of water and has problems with paraffin.

So far, we have met with LR several times and discussed well plans. A Bass Islands oil sample was received from LR for laboratory testing. Our plans for this task are to gather past and future production data from this well and establish a baseline. Finally, we will test the equipment in their well for approximately one year.

2.4.6 Oil Wells Under Water-Drive

The operator involved in this subtask of the project is East Resources (ER). ER is located close to Pittsburgh, Pennsylvania and has several Gordon formation waterflooding operations in Pennsylvania and West Virginia. The Gordon formation is a sandstone bed that has been produced for over 100 years.

Presently, most of the ER wells have electricity. Measurement consists of wells grouped into common tanks. Paraffin is a big problem for ER. Water production cuts range from 10% to 90%.

To date, we have spoken to ER several times. ER has several thousand wells for us to choose from. Well options include openhole completion, cased-through and perforated, injection, secondary production, and primary production outside the waterfloood. Our next step is to jointly choose a group of wells for the project. Next,

these wells will need separate fluid measurement to record oil, water and natural gas production. Following at least three months of production baseline data, we will test the equipment in their wells for approximately one year.

3.0 Statement of Work for Year 2

3.1 Task 1. Laboratory-Scale Experiments

The system components for the slim-tube set-up (high pressure pumps and permeameters) will be delivered in the last quarter of the first year. Once this is received, assembly and testing of the set-up will be carried out.

For Year 2, we propose to carry out the following tasks:

First Quarter

1. Task 1.1: Single phase flow experiments in a tube subjected to acoustic pulse. The objective of the study which will include concurrent and countercurrent flow arrangements, will be to establish if the application of sound enhances single phase flow. Water with varying degrees of dissolved oxygen and a crude oil samples will be used in these tests. The results will be used in model verification.

Second and Third Quarters

2. Task 1.2: The slim tube will be packed with glass beads of varying size and the flow of water, brine, water-oil mixtures will be determined as a function of power input, operational frequency, duty cycle, etc. These tests will be operated under non-cavitating and cavitating conditions. The objective of the tests will be to delineate the operating regime that results in enhanced flow in porous media. During these tests, the temperature, static pressure and acoustic pressure profiles will be recorded along the column axes. The data generated is needed in 1-D model verification.

Third and Fourth Quarters

3. Task 1.3: Slab experiments will be initiated in the third quarter of year 2 to study the propagation of sound waves in two dimensions. The objective of these sets of experiments is to extend the process observed during the slim-tube experiments to two-dimensional space and attempt to replicate the field application configuration. The slab will be a thin-packed bed with a well bore in the middle. Wave propagation will be monitored across two-dimensional space using hydrophones. Other processes will be similar to the slim-tube experiments in terms of materials and liquids.

3.2 Task 2. Development of a Computer Model for Scale-up

During the last year most of the modeling efforts were focused on building the numerical framework required for solving the system of partial differential equations governing acoustic wave propagation in the porous medium. During Year 2, the numerical algorithms developed will be applied to acoustic wave interaction with porous media fluid flow. This will start with the derivation of the governing equations with appropriate constitutive relationships. The necessary constitutive equations will be formalized in the first two quarters. The numerical handling of these source terms will be done simultaneously so as to ensure synergy between the laboratory work and the simulation efforts. The work planned is divided into a number of sub-tasks described below. The timeline for executing each of the tasks is shown in the schedule below.

Task 2 Schedule

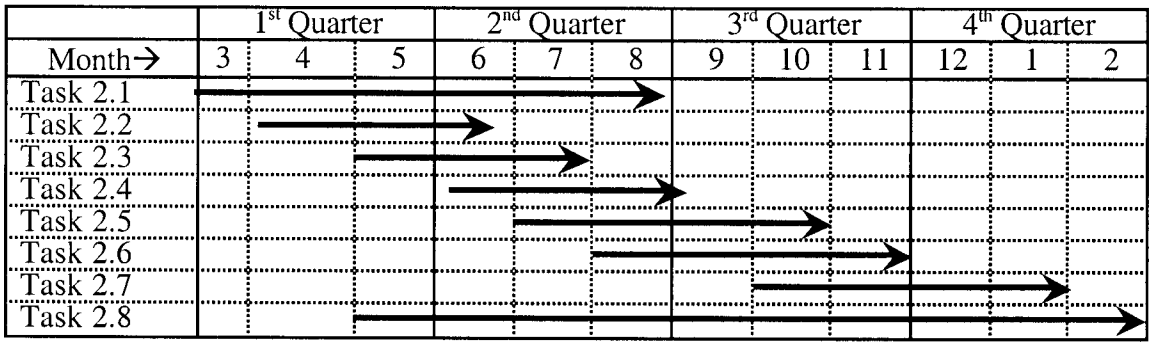

Task 2.1 Development of Constitutive Relationships

1. *Thermodynamic Consideration*

   This model must be developed to handle the physical property response of the fluid to the acoustic energy being transmitted through it. The inputs for this model are the composition of the flowing fluids and the prevailing pressure and temperature.

2. *Interfacial mass transfer terms*

   This term describes the rate of mass transfer between the flowing phases. It will be obtained from the temporal and spatial variations of the phasial weight fractions.

3. *Stress tensor evaluation*

The evaluation of this term is required for the momentum equations. These terms describes the forces acting on an element of each fluid phase. The focus would be on the surface forces.

a. *Surface forces*
    i. Internal fluid shear forces resulting in viscous dissipation of fluid momentum due to the interaction between the stationary porous medium and flowing fluids
    ii. Interphasial drag forces occurring at the interface due to the different velocities of flowing phases.

4. *Source terms resulting from cavitation*

Cavities created by the rupture of liquids under the tensile forces resulting from the propagation of acoustic pulses through the fluid body need to be quantified so that their effects on fluid transport can be modeled. In other words, the net number of cavities created or destroyed under a given pressure and temperature condition is needed.

5. *Other terms required by the energy equation*

Terms associated with interfacial mass and momentum transfer, as they pertain to the source term in the energy equation need to be formulated. Algorithms for handling terms dealing with the heat transfer between the phases and the surrounding rock matrix as well as the latent heat due to phase change will be developed.

On the simulation front the goal this year is to complete the modeling of flow experiments being conducted in the laboratory. The plan is to start with simple systems and progressively add complexity to eventually replicate the real-life situation. Along this line, the following suite of numerical experiments is proposed in increasing order of complexity.

Task 2.2 Slim Tube Experiment I

A slim tube filled with water is subjected to an acoustic pulse. Preliminary laboratory experiments have shown acoustic stimulation of tap water in a tube due to cavitation. The simulation of these experiments and the fine-tuning of the model to produce good agreement between simulated and measured results is the first modeling task required. The goal is to study the parameters that influence the simulated results in order to produce a match with the laboratory data. Parameter identification will be another objective so as to help design appropriate future laboratory experiments.

Task 2.3 Slim Tube Experiment II

A slim tube is filled with oil and is subjected to an acoustic pulse. This experiment differs from the previous one because of the differing fluid properties such as density, viscosity and interfacial tension.

Task 2.4 Slim Tube Experiment III

A slim tube is filled with two-phase oil and water and is subjected to an acoustic pulse. The objective here is to study the hydrodynamics of the multiphase flow. The added complexity pertains to relative phasial motion of the two phases.

Task 2.5 Slim Tube Experiment IV

A slim tube packed with glass beads and filled with water is subjected to an acoustic pulse. The objective here is to study the propagation of this pulse through the porous media that is represented by the packed glass beads. This will allow the incorporation of the effect of rock matrix on the impact of acoustic wave on fluid movement.

Task 2.6 Slim Tube Experiment V

Tube packed with glass beads and filled with oil is subjected to an acoustic pulse. Here the thermo-physical properties of oil and its interactions with waves in the porous medium will be studied.

Task 2.7 Slim Tube Experiment VI

A slim tube packed with glass beads and filled with two-phase oil and water is subjected to an acoustic pulse. The ultimate objective of slim tube modeling of the porous medium will be achieved by this modeling effort.

Task 2.8 2-D Slab experiments VII

The construction of the model to simulate the 2-D effects within the porous medium will be commenced. The modeling effort will follow the same line as the as the slim tube modeling. Starting with the single-phase water model, followed by the single-phase oil, and finally the two-phase oil and water model will be applied.

3.3 Task 3 Development of a New Generation of Acoustic Transducers

Future work will primarily include using a Wilcoxon shaker, F4/F7, to supply a broad range of drive frequency of 10 to 20,000 Hz. This shaker is designed to generate

broadband signals for laboratory testing. The objective is to investigate the physics of sonication of oil saturated cores as a function of frequency as well as amplitude. A housing is being fabricated to mount the shaker and couple it to the slim tube. A hydrophone will be placed in a housing attached at the opposite end of the tube. This hydrophone will monitor the signal that penetrates the core sample. Tubes will be of variable length and width and internal diameter and each will be dedicated to specific core sample. A computer control data acquisition system will be used to acquire the projector and hydrophone voltages as well as other pressure, temperature, and vibration data.

3.4 Task 4. Field Testing of the Sonication Technology

The overall plan for Task 4 is to perform field trials of the sonic transducer design. These trials will take place in production and/or injection wells located in Pennsylvania, New York, and West Virginia. Preparation work before testing the equipment includes choosing the wells, obtaining well and production records, setting up individual well measurement of production fluids, and establishing a production baseline. The second year plan for Task 4 of the project consists of the following.

First Quarter

- **General**
  - Continue to work on an in-depth description of the geological formations that are being studied and the enhancement that sonication will provide to production;
  - Determine the geological context of the reservoir; and
  - Obtain the typical decline curves.

- **Subtask 4.1. Evaluation in Partially Depleted Sandstone**
  - Obtain production data to generate production baseline for four new Glade/Clarendon formation wells

- **Subtask 4.2. Evaluation in a Shot Hole**
  - Meet with producer to choose Glade/Clarendon formation shot well.

- **Subtask 4.3. Evaluation in a Hydro-fractured Wellbore**
  - Meet with producer to choose Glade/Clarendon hydro-fractured well.

- **Subtask 4.4. Evaluation in a Fractured Carbonate**
    - Meet with producer to visit well site, obtain well records and obtain past production records for Bass Islands well.

- **Subtask 4.5. Oil Wells Under Water-Drive**
    - Meet with producer to choose Gordon formation water-drive wells.

Second Quarter

- **General**
    - Continue to work on an in-depth description of the geological formations that are being studied and the enhancement that sonication will provide to production;
    - Determine the geological context of the reservoir; and
    - Obtain the typical decline curves.

- **Subtask 4.1. Evaluation in Partially Depleted Sandstone**
    - Obtain production data to generate production baseline for four new Glade/Clarendon formation wells.

- **Subtask 4.2. Evaluation in a Shot Hole**
    - Develop an equipment plan for measuring oil, water, and natural gas production for the well; and
    - Meet with producer to visit well site, obtain well records and obtain past production records for Glade/Clarendon formation well.

- **Subtask 4.3. Evaluation in a Hydro-Fractured Wellbore**
    - Develop an equipment plan for measuring oil, water, and natural gas production for the well; and
    - Meet with producer to visit well site, obtain well records and obtain past production records for Glade/Clarendon formation well.

- **Subtask 4.4. Evaluation in a Fractured Carbonate**
    - Obtain production data to generate production baseline for Bass Islands formation well.

- **Subtask 4.5. Oil Wells Under Water-Drive**
  - Develop equipment plans for measuring oil, water, and natural gas production for individual wells;
  - Obtain well records; and
  - Obtain production history for all wells.

Third Quarter

- **General**
  - Continue to work on an in-depth description of the geological formations that are being studied and the enhancement that sonication will provide to production;
  - Determine the geological context of the reservoir; and
  - Obtain the typical decline curves.

- **Subtask 4.1. Evaluation in Partially Depleted Sandstone**
  - Obtain production data to generate production baseline for four new Glade/Clarendon formation wells.

- **Subtask 4.2. Evaluation in a Shot Hole**
  - Install equipment for measuring oil, water and natural gas production for well.

- **Subtask 4.3. Evaluation in a Hydro-Fractured Wellbore**
  - Install equipment for measuring oil, water and natural gas production for well.

- **Subtask 4.4. Evaluation in a Fractured Carbonate**
  - Obtain production data to generate production baseline for well.

- **Subtask 4.5. Oil Wells Under Water-Drive**
  - Install equipment for measuring oil, water and natural gas production for individual wells.

Fourth Quarter

- **General**
  - Continue to work on an in-depth description of the geological formations that are being studied and the enhancement that sonication will provide to production;
  - Determine the geological context of the reservoir; and
  - Obtain the typical decline curves.

- **Subtask 4.1. Evaluation in Partially Depleted Sandstone**
  - Obtain production data to generate production baseline for four new Glade/Clarendon formation wells.

- **Subtask 4.2. Evaluation in a Shot Hole**
  - Install equipment for measuring oil, water and natural gas production for well; and
  - Obtain production data to generate production baseline for well.

- **Subtask 4.3. Evaluation in a Hydro-Fractured Wellbore**
  - Install equipment for measuring oil, water and natural gas production for well; and
  - Obtain production data to generate production baseline for well.

- **Subtask 4.4. Evaluation in a Fractured Carbonate**
  - Obtain production data to generate production baseline for well.

- **Subtask 4.5. Oil Wells Under Water-Drive**
  - Install equipment for measuring oil, water and natural gas production for individual wells; and
  - Obtain production data to generate production baseline for wells.

4.0 References

Le Veque, R.J, and Yee, H.C.: "*A Study of Numerical Method for Hyperbolic Conservation Laws with Stiff Source Terms*," J. Computational Physics, Vol. 86, pp.187-210, (1990).

Roe, P.L.: "*Upwind Differencing Schemes for Hyperbolic Conservation Laws with Source Terms*," *Proc.* First International Conference on Hyperbolic Problems, Raviart and Serre (Editors), Springer, (1986).

Venkitaraman, A, Roberts, P. M., and Sharma, M. M. (1994) Ultransonic removal of near-wellbore damage caused by fines and mud solids. *Society of Petroleum Engineering and Completion*, (September), 441-444.

Appendix A. Literature Review of the Influence of Acoustic Energy on Permeability of Porous Media

Numerous laboratory studies have demonstrated the feasibility of the application of acoustic energy for the enhancement of fluid flow in porous media and remediation of wellbore damage. Comprehensive laboratory investigations conducted by U.S. and Russian scientists has been summarized by Beresnev and Johnson (1994). Table A.1 consists of the chronological summary of Beresnev and Johnson's review (case history 1-19) and a few additional studies thereafter (case history 20-24). Generally, effects such as improved permeability caused by acoustic interaction were observed in the investigations. The table also shows important experimental variables that are missing. Seventeen percent of all cases did not state the frequency or range of frequencies applied and the resulting sonic field obtained. Thirty percent of the investigators did not report the sonication irradiation time. Most workers did not report the life span of the post excitation effects where situation necessitates them. Two differing ideas emerged from acoustic energy interaction in the literature. Some workers inferred that acoustic energy interaction is indifferent to the observed permeability (Poesio et al., 2002). The majority concurred, however, that acoustic energy has positive effects, which isincreased/improved permeability of the media (Table A.1). The proposed governing mechanisms are:

- Wettability changes;
- Coalescence of oil droplets;
- Surface tension changes;
- Cavitation;
- Acoustic streaming;
- Radiation pressure;
- In pore turbulence;
- Viscosity decrease due to acoustic energy dissipation; and
- Reduction in adherence between pore wall and liquid.

Limited experimental details has resulted in knowledge gaps, lack of technology advancement, and unknown economic feasibility of using sonication technology for enhancing fluid flow and wellbore damage remediation of deposit solids. The influence of different factors on the output power transferred to the test medium is rarely investigated. Power input to the system being investigated is often reported as the manufacturer's maximum rating for acoustic transducers, instead of the power dissipation into the reaction itself. Poesio et al., (2002) and Gollapudi et al., (1994) used the power output setting of their equipment to gauge the transmission of acoustic waves through Berea sandstone core

samples and ultrasonic cleaning in fluids. Wilkey et al., (1999) only reported frequency and maximum power rating of the projector used. Venkitaraman and Sharma (1994) give great details on the effect of sonic energy on the removal of fines and mud solids near wellbore; but a limited and incomplete description of the acoustic system or phenomena that give rise to that effect were missing. The treatment depth of 2.5 inches was ascribed to the acoustic stream phenomenon and less extent to cavitation.

It is nearly impossible to compare and reproduce the abovementioned results because nebulous details of applied acoustic parameters, experimental variables, and methodologies used by various workers were provided. The power output attained in a medium increases with the amplitude of ultrasonic waves and hydrostatic pressure, but decreases with increasing temperature. Factors that can influence projector/transducer power dissipation to a system include duty cycle, mode of operation (pulse/continuous wave), pulse length, amplitude and type (magnetic/piezoceramic). Hydrophones used must also be calibrated in free field/near filed conditions. Finally, changes in the physical properties of fluid: composition, viscosity, temperature and density must be stated.

References

Beresnev, I.A. and Johnson, P.A. (1994) Elastic-wave simulation of oil production: A review of methods and results. *Geophysics*, vol. 59, no. 6, 1000-1017.

Gollapudi, U.K., Band, S.S. and Islam, M.R. (1994) Ultrasonic treatment for removal of asphaltene deposits during petroleum production. *SPE International Symposium on Formation Damage Control*, February 710, Lafayette, Louisiana.

Gunal, O.G. and Islam, M.R. (2002) Alteration of asphaltic crude rheology with electromagnetic and ultrasonic irradiation. *Journal of Petroleum Scienc e and Engineering*, vol. 26, 263-272.

Lin, J-R. and Yen, T.F. (1993) An upgrading process through cavitation and surfactant. *Energy and Fuels*, vol.7, 1111-1118.

Poesio, P., Ooms, G. and Barake, S. (2002) An investigation of the influence of acoustic waves on the liquid flow through a porous material. *Journal of Acoustic Society of America*, vol. 111, 2019-2025.

Roberts, P.M., Venkitarman, A. and Sharma, M.M. (2000) Ultrasonic removal of organic deposits and polymer-induced formation damage. *Society of Petroleum Engineering and Completion*, vol. 15, no. 1, 19-34.

Shedid, A.S. (2002) A novel technique of asphaltene deposition treatment using ultrasonic irradiation. *Petroleum and Science Technology*, vol. 20, Nos. 9&10, 1097-1118.

Venkitaraman, A., Roberts, P.M., and Sharma, M.M. (1994) Ultrasonic removal of near-wellbore damage caused by fines and mud solids. *Society of Petroleum Engineering and Completion*, (September), 441-444.

Wilkey, M.L., Peters, R.W., and Furness, J.C. Jr. (1999) The use of advanced acoustic cavitation for applications in the oil and gas industry. *The 1999 Oil and Gas Conference Proceedings*. Sponsored by the U.S. DOE, Office of Fossil Energy, Federal Energy Technology Center (FETC) and National Technology Office (NPTO), June 28-30, Dallas, Texas.

Table A.1 Laboratory studies of the influence of acoustic energy on permeability of porous media

Case history no.	References	Observed effect caused by acoustic energy	Frequency range	Sonic field intensity	Duration of excitation	Duration of the effect after end of excitation
1	Duhon, 19964	increased oil recovery during water flooding; reduction of water/oil permeability ratio; increased flow rate into injection well	1-5.5 MHz	50W (power of projector)	6-9 hrs	
2	Nosov, 1965	decreased viscosity of Polystyrene solution	300 kHz	20-120 kW/m^2	20 mins	irreversible
3	Komar, 1967	100% paraffin removal			12.5-23.1 hrs	
4	Fairbanks & Chen, 1971	temperature dependent; increased oil percolation rate	20 kHz	150W (power of projector)		
5	Johnston, 1971	decreased viscosity of epoxy	47 and 800 kHz	80W, 50W (power of projector)	30s to 45 mins	up to 48 hrs
6	Abad-Guerra, 1976	removal of paraffin			0.5-1 hr	
7	Cherskiy et al., 1971	sharp increase in sample water permeability	26.5 kHz	2-9 kW/m^2		several mins

Case history no.	References	Observed effect caused by acoustic energy	Frequency range	Sonic field intensity	Duration of excitation	Duration of the effect after end of excitation
8	Gadiev, 1971	increase of efficiency of oil displacement by water; decrease of surface tension of transformer oil; decrease of viscosity of polycrylamid solution	10 Hz – 15 kHz 400-800 Hz 30-60 Hz	10-40W (power of projector) 10^{-1} W/m^2	1-5 hrs	
9	Neretin and Yudin, 1981	increase of the rate of oil displacement by water	50-80 kHz	0.8-1.2 kW/m^2	6 hrs	
10	Sokolov and Simkin, 1981	decrease oil viscosity	18 kHz	8 kW/m^2	0.5-1 hr	120 hrs
11	Snarsky, 1982	frequency dependent increase of the rate of oil displacement by water	9-40 Hz	2 kW/m^2		
12	Medlin et al., 1983	increase of the rate of oil displacement by CO_2	100 Hz	10-4 W/m^2	20 hrs	
13	Ashiepkov, 1989	increase of oil percolation rate through sample	30-400 Hz	10^{-4}-10^{-3} W/m^2		

Case history no.	References	Observed effect caused by acoustic energy	Frequency range	Sonic field intensity	Duration of excitation	Duration of the effect after end of excitation
14	Dyblenko et al., 1989	increase of the rate of kerosene displacement by water	200 Hz	88 W/m^2		
15	Pogosyan et al., 1989	acceleration of gravitational separation of kerosene and water	120 kHz	10 kW/m^2	2 hrs	
16	Kuznetsov & Simkin, 1990	increase in oil mobility	1.2 Hz	10-3 W/m^2	48 hrs	
17	Simkin et al., 1991	increase in the rate of kerosene displacement by water		7.8 m/s^2 (particle acceleration in sound field)	51-92 hrs	
18	Simkin & Surguchev, 1991	coalescence of oil droplets			2 mins	
19	Gollapudi et al., 1994	removal of asphaltenes	10 kHz	250W max. power	1-3 mins	
20	Roberts et al., 1994	removal of fines and mud solids from contaminated cores	20-80 kHz	20-250 W/m^2	3-25 hrs	
21	Venkitaraman & Sharma, 1994	reduce formation of near-wellbore damage caused by fines and mud solids	10-100 kHz 20 kHz	3.7 W/m^2 62.5 W/m^2		

Case history no.	References	Observed effect caused by acoustic energy	Frequency range	Sonic field intensity	Duration of excitation	Duration of the effect after end of excitation
22	Wilkey et al., 1999	$BaSO_4$ scale removal >90% success	20 kHz	20 W/m^2	15 mins	
23	Roberts et al., 2000	removal of paraffin	20-36 kHz	100-1,800 W/m^2	2.4 hrs	
24	Poesio et al., 2002	decreased pressure gradient; permeability remained constant	20 and 40 kHz	2 and 0.7 kW		
25	Lin & Yen 1993	Asphaltene dispersion in surfactants		6 W (projector max. power)		
26	Gual & Islam 2000	Decreased oil viscosity in water- asphaltene solution	10 kHz	250 W (projector power)		
27	Shedid 2002	Increased permeability of asphaltene damaged core; decreased oil viscosity with solvent addition	10, 15, and 20 kHz		5 to 30 minutes	

Appendix B. Literature Review of Production Formations

Glade Formation

Introduction

The following information was taken from Mineral Resources Report M52 entitled "Oil and Gas Geology of the Warren Quadrangle, Pennsylvania." This document was published in 1965 by William S. Lytle of the Pennsylvania Geological Survey. Additional information was found in Mineral Resources Report M53 entitled "Oil and Gas Geology of the Youngsville Quadrangle, Pennsylvania." This document was published in 1964 by William G. McGlade of the Pennsylvania Geological Survey.

The Warren and Youngsville quadrangles are located in Warren County of northwestern Pennsylvania. The Warren quadrangle area is about 222 square miles. About one third is productive of oil and gas. The main producing sands are the Glade, Clarendon Stray, Clarendon, Gartland, and Cherry Grove of Upper Devonian age. The Youngsville quadrangle occupies the north-central portion of Warren County adjacent to the New York State Line. As of September 30, 1963, approximately 535 oil wells and/or gas wells were producing from the Glade sandstone in the Youngsville quadrangle. The first wells were drilled in this area as early as 1865.

The term "sand" in this report refers to potentially productive zones of mostly sandstone with associated siltstones and shales. The terms "formation" or "rocks" in this report are more inclusive than the term "sand" and include transitional zones above and below the producing zone. The term "sandstone" refers only to beds of lithified sand.

Glade Formation

In the Warren quadrangle, the top of the Glade rocks lies at about 200 feet below the base of the "Pink Rock" or 75 feet below the base of the Warren Second sand. These rocks extend about 125 feet to the top of the Clarendon formation. The base of the Glade formation is also the base of the Conneaut Group and the top of the Canadaway Group, and is separated from the overlying Warren Second sand by approximately 75 feet of shale, sandstone, and siltsone. The Glade formation strata may be subdivided into three lithologic units (top to bottom): Glade siltstone, Glade sandstone (the producing zone) and the Glade transitional zone. The lower unit usually has a shale body at the base for convenient separation from the underlying sandy Clarendon formation.

The top of the Glade siltsone is the beginning of a silty section about 100 feet below the Warren Second sand. This predominantly greenish-gray slightly calcareous, argillaceous siltstone contains fossils and some interbedded greenish-gray shale. The Glade siltstone is about 40 feet thick. In areas where the Glade sand reaches maximum thickness, the sand extends upward and replaces part of the Glade siltstone. Over most of the oil and gas producing area the Glade siltstone is a consistent lithologic unit. The top of the Glade siltstone can readily be found from samples and on geophysical logs.

The middle zone is the Glade sand which is one of the main producing zones of the Warren quadrangle. This sand is mostly a very fine- to fine-grained, light-gray sandstone. In some productive areas the Glade is a greenish-gray siltstone and is also slightly micaceous and calcareous. Fossil fragments can be found in the middle of the sandstone occasionally. The productive Glade sandstone of the Glade formation in the Youngsville quadrangle occurs as a bar-like sandstone body which trends slightly east of north direction through the eastern portion of the quadrangle. This sandstone appears to thin gradually between the town of Sugar Grove and the southeastern end of the quadrangle. A thicker Glade sandstone, thought to be the same unit, seems to continue northward into Chautauqua County, New York.

Historical Review

In 1881, an oil well presumed to be from the Glade sandstone was completed near Youngsville. A considerable number of wells were drilled between 1910 and 1915 in Youngsville, Matthews Run, and in the Five Points area. After 1915, activity tapered off for several years. The Sugar Grove Gas Pool was drilled in 1925 and 1926. Almost all of the wells were either abandoned or became inoperative by the late 1920's except the wells in the Youngsville Pool and the Sugar Grove Gas Pool. Drilling was resumed in the Youngsville Pool and the Five Points Pools about 1929. In both these pools a pilot re-pressuring project was attempted. The projects were abandoned after no success. Sparse drilling continued in the Five Points Pools until 1946. Drilling activity was vigorously renewed in 1946 and about 30 wells were drilled during the year in the Sugar Grove, Five Points, and Chandlers Valley Pools. Between 1947 and 1962 operators drilled several wells each year in the Youngsville-Sugar Grove Field.

In 1949, a pilot re-pressuring project was conducted near Sugar Grove. Selected portions of the Glade sandstone were shot with nitroglycerine and then subjected periodically to injection pressures of 350 pounds per square inch during the following three years. Very little gas was injected and no increase in oil production was obtained.

Before 1962, shooting with nitroglycerin was the accepted method of completion in the Glade reservoir and all other reservoirs in the Youngsville quadrangle. Two wells within the Sugar Grove Pool were hydraulically fractured before 1953 using kerosene and sand. Neither well responded to the treatment. The use of hydraulic fracturing as a stimulation method in the Sugar Grove Pool was suspended for more than ten years.

During October, 1961, the United States Bureau of Mines, in cooperation with Howard Curtis and Son Co., cut and analyzed a 4-inch diameter rotary air core of the Glade sandstone. The well owner was advised in January, 1962 by the Bureau of Mines that hydraulically fracturing the Glade sandstone would be advantageous. A well that had been shot with 100 quarts of nitroglycerin was fractured by Curtis. This well produced satisfactory results, leading to the future method of Glade sandstone development.

Stratigraphy

A three-well correlation among wells in Tidioute area, the Youngsville area and the Warren quadrangle shows the following thicknesses of the Glade formation.

Glade siltstone	56 feet
Glade sandstone	20 feet
Glade transitional zone	74 feet

The Glade formation of the Youngsville quadrangle is the stratigraphic equivalent of the Queen formation of the Tidioute and Sheffield quadrangles, as well as the "Eighty Foot rock" and the Glade sand pay of the Warren area. The Queen formation was named after the village of Queen located in the Tidioute quadrangle. The Glade sandstone was named from a subsurface section of an oil well located at Glade, Glade Township in the Warren quadrangle in March, 1875. One author noted that the Glade sandstone of the Warren quadrangle might correlate with the Bradford First sand in McKean County which is approximately correlative with the Cuba sandstone near Cuba, Allegany County, New York.

As of 1963, the Glade unit could be traced from a point just north of the New York-Pennsylvania border to south of the town of Tidioute, along the Allegheny River. This sandstone body was difficult to trace south of the Youngsville quadrangle due to the lack of detailed subsurface data.

The Glade siltstone is usually about 45 to 55 feet thick. Consisting mainly of light-gray to medium gray, sometimes-calcereous siltstone interbedded with thin beds of dark-gray shale, the siltstone is

overlain by a dark-gray silty shale unit. Usually about 80 feet thick, the shale unit separates the Warren Second sand from the Glade rocks.

Lithologic Descriptions of Glade "sandstone" cores
Youngsville and Warren Quadrangles, Pennsylvania
Howard Curtis and Son Co.
Sandene Lease Well No. 14

Core description by William Nabors (697-748.6) and William K. Overbey, Jr. (749-771) both of the Morgantown Petroleum Research Laboratory, Bureau of Mines, United States Department of the Interior-with modifications by W.G. McGlade.

Depth, ft	*Thickness*	
Top Bottom	*Feet*	*Lithologic description*
697.47-697.9	0.43	Shale, calcareous, dark-gray
697.9-700.0	0.1	Shale, calcareous, silty, green
700.0-705.0	5.0	Sandy shale, medium-gray
705.0-708.8	3.8	Sandstone, fine-grained, shaly, calcareous, light-gray, hard
708.8-714.0	5.2	Sandstone, fine-grained, light-gray, micaceous, hard
714.0-716.5	2.5	Sandstone, fine-grained, light-gray, hard slight oil bleeding
716.5-717.41	0.91	Sandstone, fine-grained, light-gray, hard, light oil bleeding
717.41-717.85	0.44	Sandstone, fine-grained, light-gray, hard, heavy oil bleeding
717.85-720.3	6.45	Sandstone, fine-grained, with limestone laminae, light-gray, hard, heavy oil bleeding
720.3-726.0	5.7	Sandstone, fine-grained, light-gray, hard, limestone laminae heavy oil bleeding
724.65-724.8	0.15	Shale laminae
- -725.2	-	Shale pebbles
725.4-725.55	0.15	Shale
725.75-725.95	0.2	Horizontal fractures about _ inch between fractures
726.0-726.5	0.5	Sandstone, fine-grained, light-gray, slightly micaceous, hard, irregular shale laminae, heavy oil bleeding
726.5-730.3	3.8	Sandstone, fine-grained, light-gray, hard, heavy oil bleeding
730.0-730.3	0.3	Irregular shale laminae
730.3-735.85	5.55	Sandstone, fine-grained, light-gray, hard excessive oil bleeding
732.4-735.85	3.45	Fossiliferous zone
735.85-736.49	0.64	Sandstone, very fine-grained, light-gray, bubbling oil show
736.49-739.2	2.71	Sandstone, fine-grained, light-gray, hard, slight oil bleeding
739.2-739.9	0.7	Sandstone, fine-grained, light-gray, hard, fossiliferous, slight oil bleeding
739.9-741.4	1.5	Sandstone, fine-grained, light-gray, hard, oil odor
741.4-741.8	0.4	Sandstone, fine-grained, laminated, light-gray, hard, oil show
741.8-742.8	1.0	Sandstone, fine-grained, light-gray, hard, slight oil bleeding
742.8-745	2.2	Sandstone, fine-grained, highly laminated, light-gray, hard, oil odor
745.0-746.0	1.0	Sandstone, fine-grained, silty, micaceous, light-gray
746.0-748.6	2.6	Sandstone, fine-grained, silty, light-gray, medium hard
749-754	5.0	Sandstone, fine-grained, subangular, micaceous, slightly argillaceous and dolomitic, light-gray to white. Traces of Montmorillonite clay by benzidine stain. Fossiliferous in zones

754-757	3.0	Sandstone, very fine-grained, light-gray to white, interbedded within thin shale streaks
757-764	7.0	Sandstone, fine-grained, light-gray to white, micaceous, many thin clay and shale partings, some up to 1 inch thick
764-769	5.0	Shale, sandy, medium-gray to dark-gray, micaceous, with thin sandstone interbeds up to 1 inch thick
769-770	1.0	Limestone, very sandy, medium-gray, very argillaceous, very fossiliferous
770-771	1.0	Sandstone, very fine-grained, white to light-gray, calcareous, fossiliferous

CORE ANALYSIS, GLADE SANDSTONE

Howard Curtis and Son Co., Sandene Lease Well No. 14
Northwest Section 3, Youngsville quadrangle
Sugar Grove Township, Warren County, Pennsylvania

Date cored: October, 1961
Cored interval: 697'-775' Core recovery: 77.5'
Type of core: 4 inch rotary Coring fluid: air

Depth ft.	*Air permeability md. Horiz*	*Vert*	*Porosity % bulk vol*	*Saturation, percent pore space Oil*	*Water*	*Gas*	*Oil content bbl/ac ft*	*Water content bbl/ac ft*	*Salinity equiv. NaCl ppm.***
700.8	<0.1	<0.1							74,000
701.1	<0.1	<0.1	.8						
701.8	<0.1	<0.1	1.0						80,000
702.3	<0.1	<0.1	2.9						
703.2	<0.1	<0.1	.7						80,000
704.1	<0.1	<0.1	2.2						70,000
704.8	<0.1	<0.1	1.5						81,000
705.5	<0.1	<0.1	.7						91,000
706.2	<0.1	<0.1	2.8						
706.9	<0.1	<0.1	1.6						78,000
707.9	<0.1	0.1	1.2						
709.0	1.0	0.9	11.7	14.1	23.9	62.0	128	217	
709.9	0.9	1.3	11.2	15.3	19.9	64.8	133	173	205,000
710.4	1.1	0.8	12.6	25.4	26.8	47.8	248	262	
711.0	<0.1	<0.1	3.5	23.5	27.6	48.9	64	75	
711.7	0.3	0.2	10.9	31.0	29.0	40.0	267	245	98,000
712.5	0.6	0.4	12.3	20.2	23.3	56.5	193	222	
713.3	1.4	0.9	13.7	17.5	17.5	65.0	186	186	
714.2	1.1	0.9	12.9	19.3	19.6	61.1	193	196	105,000
715.0	0.8	0.8	13.3	15.7	24.1	60.2	162	249	
716.0	0.7	0.5	12.3	23.6	21.0	55.4	225	183	88,000
716.6	0.8	0.6	12.1	19.4	25.5	55.1	182	239	
717.9	<0.1	<0.1	5.0						98,000
718.8	<0.1	<0.1	5.1						
719.9	<0.1	<0.1	10.7	29.4	36.0	34.6	244	309	89,000
720.7	0.1	0.1	10.0	38.7	42.6	18.7	300	330	
721.4	<0.1	<0.1	7.6	34.9	49.2	15.9	206	290	87,000
722.1	<0.1	<0.1	9.8	19.6	38.8	41.6	149	295	
723.1	<0.1	<0.1	8.1	44.5	50.5	4.6	280	317	87,000
723.8	<0.1	0.1	1.9						

724.8	0.3	0.2	11.7	25.2	26.7	48.1	229	242	111,000
725.5	0.3	0.2	11.5	25.4	23.7	50.9	227	211	
726.2	<0.1	0.1	10.2	33.6	34.7	31.7	266	275	88,000
727.1	<0.1	<0.1	10.8	33.6	24.1	42.3	282	203	
728.2	<0.1	<0.1	2.2						
729.2	<0.1	0.1	1.5						
730.2	0.4	0.1	11.7	28.7	28.1	43.2	261	255	92,000
731.0	0.5	0.4	12.2	26.5	27.8	45.7	251	263	
731.7	0.4	0.4	12.0	27.7	25.8	46.5	258	240	95,000
732.8	0.3	0.3	11.4	30.6	23.2	46.2	271	205	
733.5	0.3	0.2	11.7	31.6	28.5	39.9	287	259	101,000
734.5	0.5	0.4	12.6	28.2	25.1	46.7	276	245	
735.6	<0.1	<0.1	2.0						192,000
736.3	0.1	<0.1	9.7	40.1	32.3	27.6	302	243	
737.1	0.5	0.5	12.4	19.8	26.9	53.3	191	259	94,000
738.0	0.7	0.6	12.4	27.3	26.3	46.4	263	253	
738.7	0.2	0.1	10.1						
739.4	0.7	0.5	12.7	34.7	21.3	44.0	342	210	109,000
739.8	0.5	0.5	12.6	27.7	28.0	44.3	271	274	
740.8	0.5	0.5	12.1	25.8	27.3	46.9	242	256	
741.8	0.6	0.5	12.5	28.3	28.0	43.7	274	272	100,000
742.7	<0.1	0.1	5.7	11.4	17.3	71.3	50	77	
744.6	<0.1	0.1	3.2	39.3	58.0	2.7	98	144	90,000
745.3	0.1	0.1	9.9	33.9	38.4	27.7	260	295	
746.3	<0.1	<0.1	9.3	35.4	49.0	15.6	255	354	90,000
747.5	0.3	<0.1	9.6	29.5	54.9	15.6	220	409	
748.9	0.1	<0.1	10.5	21.7	41.8	36.5	177	341	80,000
749.8	<0.1	<0.1	4.6						
751.2	<0.1	<0.1	5.7						98,000
752.4	<0.1	<0.1	9.7						
753.6	<0.1	<0.1	0.8						89,000
756.8	<0.1	<0.1	1.1						
758.2	<0.1	<0.1	2.2						86,000
759.8	<0.1	<0.1	5.3	20.2	48.9	30.9	83	201	
762.8	<0.1	<0.1	0.6						
766.0	<0.1	<0.1	1.0						
769.1	<0.1	<0.1	8.1	5.9	15.8	78.3	37	99	
770.0	1.1	<0.1	5.5	35.9	44.9	19.2	153	192	
771.5	<0.1	<0.1	5.1	50.6	45.2	4.2	200	179	
774.8	<0.1	<0.1	1.7						
Ave values	0.3	0.2	7.4	27.2	31.3	41.4	214	238	98,000

** Core water salinity determined by leaching crushed core sample with distilled water, measuring water resistivity and converting to equivalent NaCl concentration.

REPORT OF CRUDE PETROLEUM ANALYSIS
Bureau of Mines Bartlesville Laboratory

F.C. Eaton well No. 3 | Warren Quadrangle | Item 55
710-750 feet | Tiona Field | Pennsylvania
F.C. Eaton | Glade sand | Glade Township

GENERAL CHARACTERISTICS

Specific Gravity, 0.801 | A.P.I. gravity, 45.2 degrees
Sulphur, percent, 0.15 | Color, N.P.A. No. 6
Saybolt Universal viscosity at 100 deg F, 38 sec.

DISTILLATION, BUREAU OF MINES HEMPEL METHOD

Dry distillation Barometer 745 mm. First drop, 30 C. (86 F)

Temp C	*% cut*	*Sum, %*	*Specific gravity of cut*	*A.P.I. of cut*	*Viscosity at 100 F.*	*Cloud test, F*	*Temperature F*
Up to 50	1.4	1.4}					Up to 122
50-75	2.6	4.0}	0.680	76.6			122-167
75-100	5.3	9.3	0.698	71.2			167-212
100-125	8.8	18.1	0.727	63.1			212-257
125-150	7.9	26.0	0.746	58.2			257-302
150-175	6.0	32.0	0.762	54.2			302-347
175-200	6.3	38.3	0.776	50.9			347-392
200-225	3.7	42.0	0.787	48.3			392-437
225-250	5.6	47.6	0.797	46.0			437-482
250-275	6.1	53.7	0.812	42.8			482-527
Vacuum distillation at 40 mm. Hg							
Up to 200	3.8	3.8	0.834	38.2	40	20	Up to 392
200-225	5.1	8.9	0.839	37.2	46	35	392-437
225-250	7.7	16.6	.859	33.2	69	60	437-482
250-275	5.7	23.3	.864	32.3	87	70	482-527
275-300	5.7	29.0	.879	29.3	120	90	527-572

Carbon residue of residuum, 1.6 percent; carbon residue of crude, 0.3 percent

APPROXIMATE SUMMARY

	%	Sp. Gr.	Deg API	Viscosity
Light Gasoline	9.3	0.691	73.3	
Total gasoline and Naptha	38.3	0.736	60.8	
Kerosene distillate	15.4	.801	45.2	
Gas oil	7.5	.836	37.8	
Nonviscous lubricating distillate	15.1	.842-.870	36.6-31.1	50-100
Medium lubricating distillate	6.4	.870-.886	31.1-28.2	100-200
Viscous lubricating distillate	-	-	-	Above 200
Residuum	16.3	.898	26.1	
Distillation loss	1.0			

*Published in U.S. Bureau of Mines Report of Investigation 3385

Clarendon Formation

Introduction

The following information was taken from Mineral Resources Report M52 entitled "Oil and Gas Geology of the Warren Quadrangle, Pennsylvania." This document was published in 1965 by William S. Lytle of the Pennsylvania Geological Survey. Additional information was found in Mineral Resources Report M53 entitled "Oil and Gas Geology of the Youngsville Quadrangle, Pennsylvania." This document was published in 1964 by William G. McGlade of the Pennsylvania Geological Survey.

The Warren and Youngsville quadrangles are located in Warren County of northwestern Pennsylvania. The Warren quadrangle area is about 222 square miles. About one third is productive of oil and gas. The main producing sands are the Glade, Clarendon Stray, Clarendon, Gartland, and Cherry Grove of Upper Devonian age. The Youngsville quadrangle occupies the north-central portion of Warren County adjacent to the New York State Line. The first wells were drilled in this area as early as 1865.

The term "sand" in this report refers to potentially productive zones of mostly sandstone with associated siltstones and shales. The terms "formation" or "rocks" in this report are more inclusive than the term "sand" and include transitional zones above and below the producing zone. The term "sandstone" refers only to beds of lithified sand.

Historical Review

The Tolles well was the first well drilled southeast of the Allegheny River in the Clarendon field. This well was drilled on January 13, 1878 at Bugsbee Mills, near Stoneham. Initial production from the Clarendon sand was 20 BOPD. Clarendon wells seldom had initial production rates of more than 25 BOPD.

Drilling in the Warren area continued at a fast rate from 1881 through 1895. Since 1895, drilling has been sporadic other than for waterflooding projects from the 1940's through the 1960's.

Clarendon Formation

The Clarendon Stray sand is between the base of the Glade rocks and the Clarendon sand. The Stray is around 40 feet thick. The top of the zone usually consists of about 20 feet of medium-gray shales and siltstones with rare fine-grained sandstone. When the siltstones and sandstones are well developed and productive of oil and gas in the lower 20 feet of the zone, the productive zone is called the Clarendon Stray sand. The Stray sand is a very fine- to fine-grained, light-gray sandstone. Near Big Bend the sand produces gas along the Allegheny River. Several drillers logs show the Clarendon Stray sand separated from the Clarendon sand by one-foot-thick fossiliferous cap rock. The top of the Clarendon rocks is the top of the zone of Clarendon Stray. This top averages 325 feet below the "Pink Rock."

In 1965, the Clarendon formation was the main oil-producing zone in the Warren quadrangle. The limits of the producing area were from the quadrangle south into the Sheffield quadrangle where this sand was one of the most important producers. As of 1963, only one well was productive from the Clarendon section in the nearby Youngsville quadrangle.

The true main body of Clarendon sand is more uniform than the other oil and gas producing sands in the Warren quadrangle. The sand is very fine-grained to pebbly and light-greenish-gray colored. The thickness varies from 0 to 50 feet, averaging 30 feet. The Clarendon contains very little interbedded shale. The productive area consists of one foot to an occasional eight feet of cap rock at the top, below which gas and then oil is found in the upper 10 feet. The sand is free from

salt water. The Clarendon formation includes all sandy beds between the Glade formation above and a shale zone below which separates them from the underlying Speechley formation. When the Clarendon Stray sand is included with the Clarendon sand the interval from the base of the "Pink Rock" is 345 feet, whereas the interval from the base of the "Pink Rock" to the top of the true Clarendon sand is 365 feet.

The sandstone zones within the Clarendon formation are usually more erratic and thinner than the sandstone beds in the Glade formation. Several wells south of Youngsville show individual sandstone beds up to 6 feet thick. Cuttings from a well in the southeastern portion of the Youngsville quadrangle show about 11 feet of very fine-grained, silty, light-gray sandstone with traces of fine- to medium-size grains scattered throughout.

The Clarendon sand is best developed in the southeastern section of the Warren quadrangle where the main producing belt attains a width of over five miles. The Clarendon sand is frequently called "Third" and "Tiona" by the drillers. The base of the Clarendon is hard to determine. If the underlying Gartland is well developed, the top of the Gartland is considered to be the base of the Clarendon formation. When the base of the Clarendon rocks can be picked on the geophysical logs the lower unit of those rocks is called the zone of Clarendon sand. Approximately 40 feet thick, the zone contains the Clarendon sand at the top if developed, and shales and siltstones below.

The Clarendon formation is productive in the Morrison Run Pool, located about 4 miles southwest of Warren, Pennsylvania. This sandstone interval is usually very fine grained and light gray in color and averages about 22 feet in thickness. Sandstone beds in the Clarendon formation of the Youngsville quadrangle consist mainly of thin, very fine-grained and tight sandstone units in a predominant siltstone section.

Fields and Pools

Clarendon Field, Clarendon Pool
The Clarendon Pool, the largest pool in the Warren quadrangle, is 8 miles long and 4-1/2 miles wide. This pool trends north and south. Oil production comes from the Clarendon sand which is very fine- to fine-grained, light-gray sandstone containing some medium grains. The upper 4 to 5 feet of the sandstone unit is usually medium to very coarse grained and contains gas. The Clarendon Stray is hard to distinguish beween the Clarendon sand. The Stray lies immediately above the Clarendon sand and is separated from it at times by only a few feet of shale or by a foot of cap rock.

Clarendon Sand
Porosities, permeablilities, saturations and oil contents
Clarendon Pool
Warren quadrangle, Warren County, Pennsylvania

Pool Location	Average Porosity %	Ave Perm md	Ave Oil Saturation %	Ave Oil Saturation bbl/ac ft	Oil content bbl/ac ft
Northern End	11.1	1.01		184	10,200
Northern End	11.6	2.90		220	6,250
Middle	12.4	2.08	27.8	295	8,201
Middle	14	11.80	25.3	282	7,954
Middle	12.03	1.04	21.1	197	5,527
Southern End	10.8	21.50		278	7,370
Southern End	11	1.02		233	5,670

Lithologic description of well cuttings
Well 013, lot 488, Morrison Run Field
D.W. Franchot
Pleasant Township, Warren County, Pa.
Elevation: 1594 Ground
Total Depth: 1391 feet
Description by W.R. Wagner

Depth (Feet)	*Description of Strata*
1219	*Top of Clarendon rocks and Clarendon Stray sandstone*
1237-1246	Siltstone, 80%, coarse-grained silt to fine-grained sand, 5GY7-8/1, in small part very slightly calcareous. Shale, 20%, N6-N5, soft
1246-1248	Shale, N6, soft
1248	*Top of Clarendon sandstone*
1248-1258	Sandstone, very fine-grained sand to coarse-grained silt, medium-light-greenish-gray (5GY7/1) in part slightly micaceous, 10% slightly calcareous
1258-1260	Shale, N6, soft
1260-1265	Sandstone, similar to 1248-1258
1265-1270	Sandstone as above 40%, grading to silty sandstone. Shale, 60% soft, N6, soft
1270-1276	Siltstone, 70% soft, coarse-grained, greenish-gray (5GY6/0.5) to N6, slightly to somewhat argillaceous. Sandstone, 30%, very fine-grained, light-greenish-gray (5GY8/1-0.5), few pieces calcareous
1276-1294	Siltstone, 80%, greenish-gray (5GY6-5/1-0.5), argillaceous to somewhat argillaceous, 5-10% somewhat calcareous to calcareous, some brachiopod fragments 1289-94. Shale, 20%, N5-N4
1294	*Base of Clarendon rocks*

REPORT OF CRUDE PETROLEUM ANALYSIS
Bureau of Mines Bartlesville Laboratory

Clarendon Field	South Penn Oil Co.	Pennsylvania
Clarendon Sand, Upper Devonian	No. 38	Warren Co., Mead Twp.
981-1,006 feet	Lot 106	Warren Quadrangle

GENERAL CHARACTERISTICS

Specific Gravity, 0.785 A.P.I. gravity, 48.8 degrees Pour pt., deg F below 5
Sulphur, percent, less than 0.1 Color, N.P.A. No. 2 1/2
Saybolt Universal viscosity at 100 deg F, 36 sec.

DISTILLATION, BUREAU OF MINES ROUTINE METHOD

STAGE 1-Distillation at atmospheric pressure, 737 mm. Hg
First drop, 27 C (81 F)

Fract. No.	*Cut at* C	F	%	*Sum, %*	*Sp. Gr. 60/60 F*	*Deg API 60 F*	*C.I.*	*Aniline point C*	*S.U. Visc 100 F*	*Cloud test F*
1	50	122	5.7	5.7	0.627	94.2	-	-		
2	75	167	3.9	9.6	.659	83.2	2.3	62.6		
3	100	212	5.7	15.3	.703	69.8	13	58.2		
4	125	257	7.5	22.8	.730	62.3	17	56.0		
5	150	302	5.9	28.7	.749	57.4	18	56.4		
6	175	347	6.0	34.7	.763	54.0	18	59.0		
7	200	392	5.4	40.1	.774	51.3	17	65.0		
8	225	437	5.1	45.2	.785	48.8	17	65.0		
9	250	482	5.3	50.5	.797	46.0	17	75.0		
10	275	527	6.2	56.7	.810	43.2	19	79.0		
STAGE 2-Distillation continued at 40 mm. Hg										
11	200	392	3.0	59.7	0.823	40.4	21	84.4	42	20
12	225	437	5.1	64.8	.832	38.6	21	88.2	45	35
13	250	482	4.7	69.5	.841	36.8	22		55	55
14	275	527	4.1	73.6	.849	35.2	23		73	70
15	300	572	4.7	78.3	.858	33.4	24		115	80
Residuum			17.2	95.5	.890	27.5				

Carbon residue of residuum, 0.9 percent; carbon residue of crude, 0.2 percent

APPROXIMATE SUMMARY

	%	Sp. Gr.	Deg API	Viscosity
Light Gasoline	15.3	0.663	81.9	
Total gasoline and Naptha	40.1	0.718	65.6	
Kerosene distillate	16.6	.798	45.8	
Gas oil	8.0	.828	39.4	
Nonviscous lubricating distillate	9.7	.836-.855	37.8-34.0	50-100
Medium lubricating distillate	3.9	.855-.863	34.0-32.5	100-200
Viscous lubricating distillate	-	-	-	Above 200
Residuum	17.2	.890	27.5	
Distillation loss	4.5			

*Published by permission of Director U.S. Bureau of Mines

Gordon Formation

Introduction
The following information was taken from Mineral Resources Report M54 entitled "Oil and Gas Geology of the Amity and Claysville Quadrangles, Pennsylvania." This document was published in 1967 by William G. McGlade of the Pennsylvania Geological Survey.

The Amity and Claysville 15-minute quadrangles are located in Washington County, Pennsylvania. These quadrangles include areas of once prolific oil and gas production. The principal oil- and gas-producing reservoirs in this area are located within the Conewango Group of the Upper Devonian Series. Five major sandstone units that can be found in this group are the Hundred-Foot (Gantz-Fifty Foot), Nineveh, Gordon, Fourth, and Fifth.

Drillers' well records were the main source of rock information in the studied area in addition to geophysical logs, well samples and cores. These records were evaluated for accuracy by comparing well geological data with composite sections of different portions of the studied area. The following lists a brief description of the "dependability index" assigned to the Gordon unit.

> "*Gordon zone*.-In the Amity quadrangle, particularly in the eastern portion, the lower Nineveh may be confused with the upper part (Gordon Stray sandstone) of the Gordon zone and some difficulty may be encountered in separating the base of the Gordon from the underlying Fourth sandstone. In the western portion of the Amity quadrangle and in parts of the eastern portion of the Claysville quadrangle the Gordon Stray-Gordon separation is usually easily defined. In a large part of the Claysville quadrangle, the Gordon is a simple, undifferentiated unit while in a large part of the Amity quadrangle, the Gordon zone is multi-layered and very complex. The boundaries of the Gordon, particularly the top, are usually *dependable* but the Gordon Stray-Gordon separation is not possible when the total zone is complex."

Historical Review
In 1885, oil was discovered in the Gordon sand of the giant Washington-Taylorstown field. This sandstone reservoir would be the most prolific oil producer in the area. In 1886, a Gordon sandstone discovery of 100-170 barrels of oil per day was completed about one mile southeast of Hill Church. Intense activity followed this discovery. By 1965, very little exploration or development drilling had been carried on for many years.

Gordon Formation
The Gordon Zone is probably more complex than any other unit in the Upper Devonian of the Amity and Claysville quadrangles. In the southeastern portion of the Amity quadrangle this formation averages 90 feet thick and is a multi-layered sequence of sandstone beds. Further west where the Gordon zone is oil productive the zone is greater than 60 feet thick. The oil-producing interval is usually located at the base of the zone. Further west the sandstone beds thin and finally shale out west of the Donegal gas storage field. This storage field is located along the western edge of the Claysville quadrangle. In portions of the northeastern and central eastern portions of the Amity quadrangle the Gordon zone has usually been logged as a one or two sandstone unit. Gamma ray logs show that the zone is much thicker and very complex compared to drillers' log data. In this area the Gordon may be silty or very fine grained and therefore not recorded by the driller.

Ten to thirty feet of red and dark gray shale separate the Gordon formation from the overlying Niveneh zone. In the Claysville quadrangle and the western portion of the Amity quadrangle, this boundary is usually recognized. In the eastern portion of the Amity quadrangle where the Gordon

zone is muli-layered, the boundary may be difficult to difficult to determine without geophysical well log data.

The sandstones of the Gordon zone are white to light gray, very fine to coarse grained, with conglomerate and coarse-grained sandstones in thin beds. The roundness of grains increases with grain size. The coarser beds exhibit poorer sorting. Gray shales predominate throughout the interbedded shale sequence. However, the shales may be red near the top.

Most of the oil production is from the basal Gordon sandstone with minor amounts coming from the upper Gordon Stray sandstone unit. Gas production

Analyses of four cores

WASHINGTON OIL COMPANY
Jas. McMannis No. 9
Washington Co., PA
GORDON SANDS

2471 ft – 2500.7 ft

Sample No.	Depth in feet	Permeability Md.	Percent Porosity
GORDON STRAY			
X-1	2471.2	.23	11.82
X-2	2473.3	.68	13.21
X-3	2474.4	.44	12.63
X-4	2475.4	Impermeable	11.54
X-5	2478	Impermeable	2.63
GORDON SAND			
X-6	2492.2	2.47	13.19
S-1	2492.5	6.3	17.37
S-2	2493.0	3.62	15.24
X-7	2493.9	20.75	18.08
S-3	2494.7	26.83	19.17
X-8	2495.3	37.04	21.59
S-4	2495.9	108.32	20.59
S-5	2496.5	0.16	17.25
X-9	2497.0	182.1	22.50
S-6	2497.5	221.92	25.91
S-7	2498.0	239.69	20.00
X-10	2498.5	188.85	23.44
S-8	2499.0	284.54	28.29
S-9	2499.5	166.65	23.94

WASHINGTON OIL COMPANY
Jas. Hodgins, Sr. No. 13
Blaine Township
Washington Co., PA
GORDON SAND

Depth feet	Perm, md	Porosity, percent	Saturation percent pore volume Oil	Water	Oil content bbl/ac-ft	Chloride content of water in cores, ppm
2551.0	4.8	11.72	12.49	81.54	114	
2551.5	16.4	11.07	0.00	89.84	0	
2552.7	314.2	26.37	10.38	79.36	212	
2553.4	328.2	27.19	10.81	77.75	228	
2553.8	285.3	26.80	10.41	79.81	217	
2554.5	290.9	26.41	12.21	75.46	250	
2555.0	61.7	21.81	13.87	84.42	235	
2555.5	106.8	23.17	9.86	77.00	177	
2556.0	33.1	17.38	7.94	59.74	107	
2557.3	4.2	9.68	0.00	96.06	0	

Note: Analyzed by United States Bureau of Mines

WASHINGTON OIL COMPANY
Lemon Carson No. 10
Taylorstown Field
Washington Co., PA
GORDON SAND

Depth feet	Perm, md	Porosity, percent	Saturation percent pore volume Oil	Water	Oil content bbl/ac-ft	Chloride content of water in cores, ppm
2548.0	0.7	5.99	0.0	99.67	0	
2548.7	195.4	25.15	5.96	92.07	116	16461
2549.5	242.0	26.66	7.67	80.33	159	
2550.5	14.0	24.22	13.07	78.77	245	12637
2551.5	2.4	24.69	21.95	68.04	420	
2552.0	1.2	27.11	20.67	69.33	435	37376
2552.5	276.5	25.99	19.84	70.71	400	
2553.0	297.6	26.67	17.76	67.06	367	30299
Chloride content of water produced with oil, Lemon Carson No. 2						37762

Note: Analyzed by United States Bureau of Mines

CHARLES E. YOUNG AND ASSOC.
No. 1 J.L. Kenamond
Washington Co., PA
GORDON SAND

Depth feet	Perm, md	Porosity, percent	Saturation percent pore volume Oil	Water	Oil content bbl/ac-ft	Chloride content of water in cores, ppm
2527.7	0.3	2.49	25.62	72.02	50	
2428.4	0.9	2.28				
2432.5	0.3	3.62	15.89	80.41	45	
2443.1	1.5	4.47				
2448.1	0.4	3.54				
2450.0	1.0	7.87				
2452.7	0.7	4.59				
2459.5	9.6	6.57				
2462.1	11.6	11.21				
2462.7	3.9	11.19				
2462.8	96.0	10.11				
2465.7a	0.9	8.14	25.59	14.22	162	
2468.3b	2.5	11.69	24.86	27.16	226	111916
2469.6	1.9	10.31				
2470.4a	0.8	9.24	17.16	32.60	123	
2472.2	1.1	8.48				
2473.1b	0.9	9.16	14.47	45.08	103	
2475.6	3.2	7.72				
2477.1	1.0	8.37	25.80	41.95	168	129271
2478.5	71.5	7.82	22.60	13.09	137	21815
2479.5	1.1	7.68				
2484.2	0.4	4.52				
2486.0	0.4	5.55				

a Sample was not placed in air-tight container until 36 hours after its removal from core barrel.
b Sample was not placed in air-tight container until 12 hours after its removal from core barrel.

Note: Analyzed by United States Bureau of Mines

Lithologic description of cores

Washington Oil Company No. 13 Jas. Hodgins, Sr.
Blaine Township, Washington County, Pa.
Description by R.C. Stephenson

DESCRIPTION OF CORES

Core No. 1

Depth				
ft.	*in.*	*ft.*	*in.*	
2545		2546	3	Cored 1 foot 3 inches, recovered 1 foot. Recovered about 1 foot of dark gray shale showing pronounced bedding plane fracture. No sand. Drilled hard. No samples for analysis.

Core No. 2

2546	3	2547	3	Cored 1 foot, recovered 1 foot. Eight inches broken material, somewhat coarser than cuttings, composed of dark-gray shale and greenish-gray, fine sand. Fout inches sandstone, small, broken biscuits, light greenish-gray, fine, hard, tight, subangular grains, no petroliferous odor. Drilled hard. Not sampled for analysis.

Core No. 3

2547	3	2552	1	Cored 4 feet 10 inches, recovered 1 foot. Four inches broken material, somewhat coarser than cuttings, composed of dark gray shale and fine gray sand, as above, with shale fragments predominating. No biscuits. Separated from sand in lower part of core barrel by broken clayey shale packed in the barrel. Eight inches sandstone, light gray, fine, fairly hard, with random distribution of small, well-rounded pebbles. A few small biscuits and much pulverized sand. Quite strong petroliferous odor. Samples 1 and 2 taken from this zone for analysis. At 2548 feet was a marked drilling break, probably marking the top of the Gordon Sand.

Core No. 4

2552	1	2555	4	Cored 3 feet 3 inches, recovered 3 feet 3 inches. Three feet, three inches sandstone, light gray with greenish cast, fine at top grading to medium fine below, with some pebbles in the sand near the top, slightly micaceous, becoming more soft and friable in the lower two feet. Strong petroliferous odor, with small amount of light green oil along some fresh fractures. Samples 3,4,5,6 and 7 come from this core. All of this interval drilled easily.

Core No. 5

Depth				
ft.	*in.*	*ft.*	*in.*	
2555	4	2557	10	Cored 2 feet 6 inches, recovered 2 feet 2 inches. One foot, one inch sandstone, light greenish-gray, fine, fairly soft, somewhat friable, increasing hardness toward base where there are some random pebbles scattered through the sand. Strong odor and traces of light green oil decrease downward. Nine inches, shale, dark gray, very hard.

Four inches sandstone, light gray, very fine, hard, tight, with no apparent odor on fresh fracture. Sample 10 from this interval.

Core No. 6

2557 10 2559 10 Cored 2 feet, recovered 3 inches.
Three inches sandstone, medium gray, very fine, hard, tight, with some very thin dark gray shaly streaks.

Steel line measure at 2560 feet.

Description of Gordon samples from two wells

Gulf Oil Company No. 1 Lone Pine Unit
Elevation (KB) 1244 feet
Description by W.G. McGlade

Depth (Feet)	*Sample Description*
2750-2800	Siltstone: light gray
2750-2801	Siltstone: red and Shale: dark gray TOP OF GORDON SANDSTONE
2750-2802	Sandstone: very fine to coarse grained, mostly fine grained, light gray
2750-2803	Shale: dark greenish-gray and Sandstone: as above
2750-2804	Sandstone: very fine to medium grained, light gray
2750-2805	Shale: silty, mostly red, and medium greenish-gray
2750-2806	Sandstone: very fine to fine grained, silty, light reddish-gray
2750-2807	Sandstone: very fine grained, light greenish-gray BASE OF GORDON SANDSTONE
2750-2808	Shale: silty, light gray

Charles E. Young and others, Harry Hatfield No. 1
North Strabane Township, Washington County, Pa.
Completed January, 1946
Elevation 1343 feet
Description by C.R. Fettke
(modified by W.G. McGlade)

Depth (Feet)	*Sample Description*
2650-2668	Shale, dark gray, with some interbedded very fine to fine-grained light gray sandstone and a little purplish-red silty shale
2668	Top of Gordon Sand
2668-2690	Sandstone, fine-grained, light gray, with considerable interbedded gray shale
2690-2700	Sandstone, very fine-grained, light gray, with a great deal of interbedded gray shale
2700	Bottom of Gordon sand
2700-2742	Shale, dark gray, with a little interbedded very fine-grained, light gray sandstone

Analysis of oil sample from the Gordon sand in the Washington Field, Washington County, Pennsylvania. Data from the "Report of Investigations, Analyses of Crude Oils from Some Fields of Pennsylvania and New York" by E.C. Lane and W.L. Gardon, January 1938, p. 58-62:

Sample 23390
W.W. Moore well no. 2
2,631-2,637 feet
Manufacturers Light & Heat Co.

Item 50
Pennsylvania
Washington County
N. Franklin Township

Washington Field

Gordon Sand

GENERAL CHARACTERISTICS

Specific Gravity, 0.800
Sulphur percent, less than 0.10
Saybolt Universal viscosity at 100 deg F, 44 sec.

A.P.I. gravity, 45.4 degrees
Color, dark green

APPROXIMATE SUMMARY

	%	Sp. Gr.	Deg API	Viscosity
Light Gasoline	0.8			
Total gasoline and Naptha	24.3	0.748	57.7	
Kerosene distillate	23.5	0.788	48.1	
Gas oil	10.2	0.827	39.6	
Nonviscous lubricating distillate	4.4	0.832-0.855	38.6-34.0	50-100
Medium lubricating distillate	3.7	0.855-0.859	34.0-33.2	100-200
Viscous lubricating distillate				Above 200
Residuum	21.7	0.889	27.7	
Distillation loss				

Akron Dolomite (Bass Islands) Trend

Introduction

The "Bass Islands Trend" is a popular name for a long (38-40 mile) narrow, (1-1/2 miles or less wide) discontinuous belt of productive oil and gas wells in portions of Chautauqua, Cattaraugus and Erie Counties, New York. The largest part extends from east of the village of Sinclairville southwest to the village of Clymer, crossing Chautauqua Lake at the narrows.

The productive formation is usually the Onondaga Limestone and occasionally the underlying Akron Dolostone. These formations are approximately 1000 feet above the Medina Group. The Onondaga is present at the surface in the Buffalo area.

The name "Bass Islands" is a misnomer that has been used by drillers in the trend. Bass Islands is a Canadian and Ohio term for the Akron-Bertie Group of New York. This group is composed of rocks just below the Onondaga Limestone.

History

National Fuel's Zoar field was the first field in the Bass Islands Trend which produced during the late 1800's until 1916 when it was converted to storage. No other Onondaga Akron production was encountered until 1963 when Wolf's Head Refining drilled a well near Ellery Center just northeast of Chautauqua Lake. Drilled as a deep test, the well penetrated through a faulted Onondaga section and some oil and gas production was reported in a zone below the unconformity separating the middle Devonian from Upper Silurian. However, the well was considered non-commercial and was plugged. In early 1981, a natural flow of gas was encountered in the Onondaga Limestone in a well at Gerry, New York. The operator overlooked the importance of the gas in the Onondaga and simply completed the Medina.

In February 1981, an operator based in Hamburg, New York drilled a well in the southwestern corner of Chautauqua County. This well was originally scheduled to be a 4500 feet Medina test well. However, the well blew out and flowed oil from a depth of 2885 feet. Before the well was brought under control, several hundred barrels of high gravity crude oil were reported to have flowed to the surface. Amazingly, this well was the first flowing oil well in the state of New York in nearly forty years from a zone not commonly recognized as productive for hydrocarbons. Numerous discoveries followed, dispelling the idea that the first was an isolated occurrence.

Bass Islands Trend

In early 1980, repetition of section in Gamma Ray logs was noticed in several Medina wells in Chautauqua County, New York. The repeated section was generally part of the interval from above the top of the Devonian Onondaga Limestone to the mid point of the Silurian Salina. Reverse faulting caused this structural complication. Wells with repeated sections often had gas and/or oil shows at the fault break. These shows were generally considered uneconomic.

Further drilling into this trend led to three conclusions. The faults are enechelon and genetically related. These faults traverse the county laterally from northeast to southwest. The faults are located in a narrow fairway about two miles wide.

Art Van Tyne of the New York State Oil & Gas Research Office mapped and showed the same trend in several 1980 publications. Mr. Van Tyne projected two parallel reverse faults that traversed Chautauqua County and continued into adjacent Catteraugus and Erie Counties. Isopach maps of the interval from the top of the Onondaga to the base of the Packer Shell across Chautauqua County show thickening in the trend area.

The Harrington #1 well in Ellery Township was drilled by Wolfshead Refining in 1963 in the trend. This well was drilled as a deep test, but was unsuccessful. A small amount of oil and gas

production was reported in a zone below the unconformity separating the Middle Devonian from Upper Silurian.